

THE RAMAN SPECTRA AND STRUCTURE OF  
SILICA AND THE SODA-SILICA GLASSES

by

GEORGE BARWICK WILMOT

B.S., Rensselaer Polytechnic Institute  
(1951)

SUBMITTED IN PARTIAL FULFILLMENT  
OF THE REQUIREMENTS FOR THE  
DEGREE OF DOCTOR OF PHILOSOPHY

at the

MASSACHUSETTS INSTITUTE OF TECHNOLOGY

Signature of Author - \_\_\_\_\_  
Department of Chemistry, Nov. 10, 1954

Certified by - - - - - Thesis Supervisor

Accepted by - - - - - Chairman, Departmental Committee -  
on Graduate Students

### Abstract

#### The Raman Spectra and Structure of Silica and the Soda-Silica Glasses

by

George B. Wilmot

Submitted to the Department of Chemistry on November 12, 1954  
in partial fulfillment of the requirements for the  
degree of Doctor of Philosophy

The Raman spectra of  $\alpha$ -quartz, vitreous silica and a series of soda-silica glasses from 9 to 44 mole percent Na<sub>2</sub>O were studied. Quantitative photographic intensity measurements were made. These permitted a comparison of the total intensity of the Raman scattering of quartz with that of vitreous silica, and a study of the band intensities in the glasses as a function of composition. The interpretation of the Raman spectrum of quartz differed little from those given in the literature. Frequency and intensity distributions in the spectrum of vitreous silica were found to be different from those in the quartz spectrum at frequencies below 500 cm<sup>-1</sup>. However the total intensities of the Raman scattering of the two substances were of the same order. The continuum found in the Raman spectrum of vitreous silica in the range 100 - 500 cm<sup>-1</sup> was interpreted to indicate that any microscopic order cannot extend over dimensions larger than a few times the unit-cell size of quartz.

In the spectra of the soda-silica glasses, the bands associated with the three-dimensional silica network (as found in vitreous silica) decreased progressively in intensity with increasing soda content. Conversely bands associated with various kinds of Si-O<sup>-</sup> linkages progressively increased in intensity. Frequencies have been assigned to stretching and bending modes of the Si-O<sup>-</sup> groups. Agreement between the Raman frequencies of the soda-silica glasses and the published infrared frequencies is rather poor. It is not apparent whether this disparity is due to experimental causes or has a more fundamental origin such as pseudo-symmetry which causes strongly Raman-active modes of vibration to be weak in the infrared and vice versa.

Harper (Chem.) Nov. 22, 1955

Thesis Supervisor: Richard C. Lord  
Title: Professor of Chemistry

This thesis has been examined by:

1.....

2.....

3,.....

4..... Chairman

5..... Thesis Supervisor

#### **ACKNOWLEDGEMENTS**

The author wishes to express his thanks and indebtedness to Professor R. C. Lord for his constant guidance throughout the course of this investigation. The financial aid given by the M.I.T., Department of Chemistry and the Owens-Illinois Glass Company is gratefully acknowledged. Thanks are due to the personnel of the Research and Development Laboratories of the Owens-Illinois Glass Company who prepared the samples and to A. Campbell, N. Nicholson and G. W. Prince of the Chemistry Department Shops for valuable assistance in the design and construction of the apparatus.

## TABLE OF CONTENTS

	page
I. Introduction.....	1
II. Experimental.....	5
A. Samples.....	5
B. Equipment and Techniques.....	9
C. Results of Measurements.....	15
III. Discussion of Results.....	30
A. Raman Spectrum and Structure of $\alpha$ -Quartz.....	30
B. Raman Spectrum of Vitreous Silica.....	42
C. Raman Spectra and Structure of the Soda-Silica Glasses.....	52
IV. Summary of Structural Conclusions about Silica and the Soda-Silica Glasses from Infrared and Raman Spectra - Suggestions for Future Work.....	62
Appendix I - Design Operation and Performance of the Excitation Unit.....	65
Appendix II - Details of Intensity Measurements.....	71
Appendix III - Study on Cristobalite.....	76
Bibliography.....	81

## TABLE OF FIGURES

- Fig. 1 The Raman Spectrum of Quartz.....17  
Fig. 2 Comparison of the Raman Intensities of Quartz and Vitreous Silica.....following 19  
Fig. 3 Raman Spectrum of Quartz below 500 cm<sup>-1</sup> as Recorded Photoelectrically.....21  
Fig. 4 Raman Spectra of the Soda-Silica Glasses....22  
Fig. 5 Symmetry Modes of Quartz.....following 40  
Fig. 6 Drawing of Excitation Unit.....following 66  
Fig. 7 Circuit Diagram for Mercury Arc Power Supply.....following 67  
Fig. 8 Fine Structure of the Totally Symmetric Vibration ( $\nu_1$ ) in CCl<sub>4</sub>.....following 69  
Fig. 9 Typical Calibration Curve for 103a-0 Plate....  
.....following 74

## I. Introduction

Recent work by Simon and McMahon<sup>35,36</sup> on the infrared spectra of silica and the soda-silica glasses has indicated that the study of the vibrational spectra of vitreous materials promises to aid the understanding of the structure of these materials. These workers found a strong similarity between the spectra of the crystalline modifications of silica, particularly that of cristobalite, and the spectrum of vitreous silica. They also studied the progressive modification of the vitreous silica spectrum as a function of increasing soda content of these binary glasses.

The purpose of the present investigation of the Raman spectrum of silica and the soda-silica glasses was to supplement and extend the infrared work of Simon and McMahon. By means of the Raman effect, the vibrational frequencies can be studied over the entire frequency range. In addition, a study of the Raman spectra might uncover new bands even in regions accessible to infrared study since it is known that several of the strongest Raman bands in the crystalline forms of silica are infrared inactive. Hence the corresponding bands in vitreous silica might be expected to be very weak (and hence undetectable) in the infrared. This is particularly true since the infrared study was a study of the reflection spectra. This method is incapable of detecting weak bands.

Prior to the initiation of this research, the only published Raman study of glasses of simple, known compositions was that of Vuks and Ioffe<sup>40</sup> who studied the spectra of a series of soda-silica glasses ranging from 73 to 50 mole % silica. They found only four bands in each glass and no bands below 530 cm<sup>-1</sup>.

Since the Raman spectrum of vitreous silica extends at least down to 250 cm<sup>-1</sup>, it was felt that a study of glasses of higher silica content would be helpful in establishing more carefully the connection between the Raman frequencies of vitreous silica and those of the soda-silica glasses. In addition the lack of agreement between the infrared data of Simon and McMahon and the Raman work of Vuks and Ioffe might be resolved.

While this research was in progress, the work of Gross and Kolesova <sup>11</sup> was published giving the Raman frequencies of the Na<sub>2</sub>O-SiO<sub>2</sub>, K<sub>2</sub>O-SiO<sub>2</sub> and Li<sub>2</sub>O-SiO<sub>2</sub> systems. Here again no glasses were studied with silica contents greater than 80 mole percent. In addition the spectra were measured visually and the intensities given were visual estimates. Because of the broad diffuse nature of the Raman bands in these vitreous materials, it is virtually essential to study the spectra by means of densitometry, both in order to measure frequencies accurately and to obtain accurate estimates of intensities.

Although the Raman spectrum of vitreous silica has been reported several times in the literature<sup>11,12,15,21,22,23,24</sup>, the results are not in complete agreement. In particular, in the region below 500 cm<sup>-1</sup>, some workers have reported several bands, while others only a single continuum. In order to determine the extent to which these discrepancies are attributable to differences in the methods of manufacture of the various samples, a study was made of samples of vitreous silica made by a variety of methods.

The Raman spectrum of quartz has been the subject of numerous investigations since the earliest days of Raman spectroscopy\*. The work of Saksena<sup>31</sup> is especially complete, giving polarization data and group-theoretical analysis. The spectrum obtained by Krishnan<sup>20</sup> was excited by the mercury line at 2537A and contains a large number of lines attributable to overtones and combination tones in addition to the spectrum usually obtained.

In view of the large amount of reliable work in the literature, it was decided not to make a complete restudy of the Raman spectrum of quartz, but to study merely those aspects, such as intensity, which have a direct bearing on the spectrum of vitreous silica.

Since the work Simon and McMahon showed that the

---

\*See Ref. 29 for extensive bibliography

spectrum of vitreous silica is more nearly like that of cristobalite than any other of the crystalline form of silica, it seemed desirable to obtain the Raman spectrum of cristobalite and, accordingly an attempt was made to excite the Raman spectrum of a finely powdered sample of cristobalite. However, this attempt proved unsuccessful. An account of the method is given in Appendix III.

## II. Experimental

### A. Samples

All samples of quartz studied were  $\alpha$ -quartz, the modification stable below 575°C. The quartz samples were in the form of rods of rectangular cross section. Two samples were cut with the optic axis parallel to the direction of observation and were 90 x 10 x 9.8 mm and 80 x 9.5 x 9 mm. The other two samples were cut with the optic axis perpendicular to the direction of observation and were 60 x 12 x 7.5 mm, and 80 x 9.5 x 9 mm. In all cases the long dimension was the direction of observation.

Three samples of vitreous silica were studied to ascertain whether the spectrum was dependent on the method of manufacture. Sample No. 1, a rod of regular commercial silica 7 mm in diameter and 150 mm in length, was obtained from McAllister-Bicknell Company.

Sample No. 2, a rod 12 mm in diameter and 120 mm in length was especially prepared by Hanovia Chemical Company for this research. It was drawn from a larger rod which was built up layer by layer by deposition of finely powdered quartz at high temperatures. According to the manufacturer, it is highly unlikely that a rod manufactured in this fashion would contain any crystalline regions resulting from incompletely fused crystalline quartz.

Sample No. 3, 56 x 9.25 x 9.25 mm, was silica of very high purity, prepared from  $\text{SiCl}_4$  by oxidation to the dioxide. This sample, since it was not prepared by the fusion of crystalline quartz, could, of course, contain no regions of crystallinity attributable to partially fused quartz.

The compositions of the samples of the soda-silica glasses are given in Table I. The samples were prepared and analyzed in the Research and Development Laboratories of the Owens-Illinois Glass Co. According to Dr. S. W. Barber<sup>3</sup> of that Company the samples were prepared as follows:

"The rods were formed by drawing up the fluid melts into the steel mold by vacuum. This produced a very drastic quench but fracture was avoided probably because the surfaces of the samples were in compression. These highly strained samples were placed in a cold annealing oven and-- except for samples 1, 2, and 3--heated to within about  $25^{\circ}\text{C}$  of the annealing temperatures used by Glaze, Young, and Finn, (NBS; Jr. of Research, 2, 799) where they were held for about 3 hours. They were then cooled overnight at a mechanically controlled rate which did not exceed about  $1^{\circ}\text{C}$  per

**Table I - Composition of the Soda-Silica Glasses Studied**

Sample No.	Mole % Na <sub>2</sub> O	Wt. % Na <sub>2</sub> O	Wt. % SiO <sub>2</sub>	Density <sup>27</sup>	Moles SiO <sub>2</sub> per cm <sup>3</sup>
1	9.01	9.27	90.73	2.274	.0343
2	12.69	13.94	86.96	2.300	.0333
3	16.05	16.48	83.52	2.327	.0324
4	25.26	25.83	74.17	2.434	.0301
5	29.0	29.7	70.3	2.460	.0288
6	33.26	33.97	66.03	2.489	.0274
7	42.82	43.60	56.40	2.522	.0237

minute. They were hot to the touch when removed from the oven and wrapped in tin foil to avoid surface damage from handling. Samples 1, 2, and 3 became bluish, evidently due to devitrification, when treated in this way. Consequently they were held for only about 1 hour at 550° (i.e. 50°C lower than the prescribed annealing temperature) and cooled as above."

For observation of the Raman scattering the rods were ground and polished on one end. As the soda content increased beyond 25%, the glasses became increasingly hygroscopic and the grinding had to be carried out with glycerine as a grinding fluid. Polishing proved possible with rouge and small amounts of water.

The samples containing less than 25% Na<sub>2</sub>O were 11 mm in diameter, while those above 25% Na<sub>2</sub>O were 8 mm in diameter. The lengths of the rods varied from 8 to 10 cm.

Visual examination indicated a considerable lack of homogeneity in the form of waviness which decreased with increasing soda content. In most cases the Raman spectra were excited with the glass rods surrounded by "Nujol" to minimize scattering of light by the irregular surfaces of the glasses and to protect the glasses from atmospheric water vapor.

### B. Equipment and Techniques

The earlier part of the work was concerned with the measurement of the Raman frequencies of the various samples, long exposure times being used to bring out the weak lines. For this work the spectra were excited in a unit containing six General Electric AH-2 type mercury arcs. The mercury line at 4358A was used for the excitation of all spectra reported in this research. Before reaching the samples the radiation was filtered through a 1 cm layer of saturated sodium nitrite solution and 5 mm layer of a concentrated solution of praseodymium chloride. The nitrite filter greatly reduces the intensity of radiation below 4200A while the praseodymium chloride removes to a considerable extent the continuum in the region 4380 to 4600A (approximately 100 to 1200  $\text{cm}^{-1}$  from 4358A). The transmission curves for these filters have been given by Stamm.<sup>37</sup> It was estimated from these curves that the transmission of the filter combination used here was about 25% at 4358A.

For these experiments, a Zeiss three prism spectrograph of aperture f/4.5 was used which gave a plate factor of about 29A/mm ( $147 \text{ cm}^{-1}/\text{mm}$ ) at 4454A ( $500 \text{ cm}^{-1}$  from 4358A).

Under these conditions, exposures of two to ten hours duration were made of the spectrum of quartz, and of 20 to 100 hours for the spectra of the glasses and vitreous

silica. Exposures of longer duration were not successful due to the high background produced by the scattering of the continuum in the mercury arc radiation.

Because of the broad, and in some cases assymmetric nature of the Raman bands in glasses, the measurement of band frequencies was difficult. Of the methods tried - visual comparison with the iron spectrum by means of a hand lens or microscope comparator, photographic enlargement, and measurement from densitometer curves - only the last proved feasible in most cases.

The densities of the bands on all good plates were measured on a Baird Recording Densitometer\*, enabling frequencies to be measured and qualitative band intensities to be assigned. The frequencies of the Raman bands of quartz were measured by interpolation between the lines of the iron spectrum which was imposed on every plate. These interpolations were made with the help of a Hilger Comparator.

Because the relatively high ratio of continuum intensity to the intensity of Hg 4358A in the spectrum of the AH-2 arcs would greatly hinder quantitative intensity measurements, especially those made photoelectrically, it seemed desirable to construct mercury arcs of the "Toronto" type.<sup>47</sup> These are direct-current arcs with water-cooled mercury-pool electrodes, and have been shown to give very little continuum.

\*We are greatly indebted to Mr. R. O. Carpenter of Baird Associates, Cambridge, Mass. for the use of the instrument.

A new excitation unit was therefore constructed employing two arcs of this type. A detailed account of the design and performance of these arcs together with a comparison of the two excitation units is given in Appendix I.

Most of the measurements of the spectra excited by this new unit were made with a fast grating spectrograph of high dispersion. The optics of this instrument have been discussed elsewhere<sup>16,31</sup> but briefly it employs an off-axis paraboloid as its collimating element and a plane grating with 30 in<sup>2</sup> of ruled area 30,000 lines/in. as its dispersing element.

A spectrum can be either photographed with an f/5.4 camera or measured photoelectrically at the exit slit. In the latter case, the instrument is a spectrometer of the autocollimating type, the spectrum being scanned by rotation of the grating.

In the second order, this instrument has a plate factor of 4.6A/mm (23 cm<sup>-1</sup>/mm) at 4500A. While this high dispersion was useful in the study of the Raman spectrum of quartz where there are sharp and closely spaced lines, the high resolution was not needed in the study of the glass spectra where the bands were broad. However, the high dispersion facilitated the measurement of the Raman frequencies even where the bands were broad. In addition, the grating

spectrograph proved to be somewhat more free of stray and scattered light than the prism instrument and consequently gave cleaner spectra. A disadvantage was the presence of grating ghosts which became evident when the sample scattered an abnormal amount of Hg 4358A. This condition was serious only in the case of glasses containing about 16% Na<sub>2</sub>O.

As the initial work on the spectra of the glasses showed striking intensity changes with increase in soda content, it became evident that quantitative measurements of the intensities would be of great value in the interpretation of these spectra. Because of the well-known difficulties of photographic photometry, it was decided to make these measurements photoelectrically using the grating spectrometer.

The amplifier and recorder available for this work had been designed to be used for the recording of fluorescent spectra, and the amplification was not sufficiently high to detect the low signals produced by the very weak light of the Raman effect. Accordingly a preamplifier was built in the electronics shop of the Laboratory of Nuclear Science and Engineering which permitted the detection of light signals whose intensities were 1/100 of the previous lower limit.

It was hoped that the spectra of the samples might be recorded photoelectrically with the new excitation unit and the improved amplifier. This proved to be possible only for crystalline quartz, in which case six or so of the strongest lines could be recorded. Although the strong bands in the glasses could be detected, the signal-to-noise ratio at the highest level of amplification proved to be so low that the band shapes and positions were greatly distorted by the noise despite the high degree of filtration used in the circuit. Thus no quantitative measurements could be made photoelectrically.

After a great deal of experimentation with excitation conditions and circuitry in an effort to improve the signal-to-noise ratio, it was concluded that successful measurements would require a photomultiplier tube of higher quality and possibly a new amplifying circuit. As neither of these was ~~im~~mediately available, it was decided to make the measurements photographically with the realization that the precision of this method would be rather low.

Exposures of seven hours duration were then taken of the spectrum of each glass on the grating instrument with the water cooled arcs as exciting sources. The details of exposure conditions and plate calibration and processing are given in Appendix II. The densities and band frequencies

were measured on a Jarrell-Ash Model JA-2305 Recording Microphotometer.\* The densities were converted into intensities by means of calibration spectra taken on each plate.

For some compositions of the glasses, polarization measurements were made using the two-exposure method of Edsall and Wilson<sup>4a</sup>. For these experiments the Zeiss spectrograph was used.

---

\*We are greatly indebted to Dr. F. Breck of the Jarrell-Ash Company, Newtonville, Mass., for the use of this instrument.

C. Results of the Measurements

The measured frequencies of the Raman lines of quartz are compared with the values recorded in the literature in Table II. It is estimated that the precision of our measurements is  $\pm 1 \text{ cm}^{-1}$ . The spectra of samples of quartz with optic axis ( $\gamma$ ) both parallel and perpendicular to the direction of observation are given in Figure 1. Figure 3 shows the spectrum of quartz as recorded photoelectrically with the optic axis parallel to the direction of observation.

The agreement between our values and the literature values is good. The weak line reported at  $479 \text{ cm}^{-1}$  by Saksena<sup>31</sup> has not been found by any other workers and probably does not exist.\* He was able to observe it only in polarization experiments in which the intensity of the strong neighboring line at  $465 \text{ cm}^{-1}$  was greatly reduced. We have examined the spectrum using sufficient dispersion to separate these two lines and have not been able to find it. Krishnan<sup>20</sup> has also examined the spectrum at high dispersion and with long exposure times. Although he has reported many weak lines not reported by Saksena, he did not find this line.

---

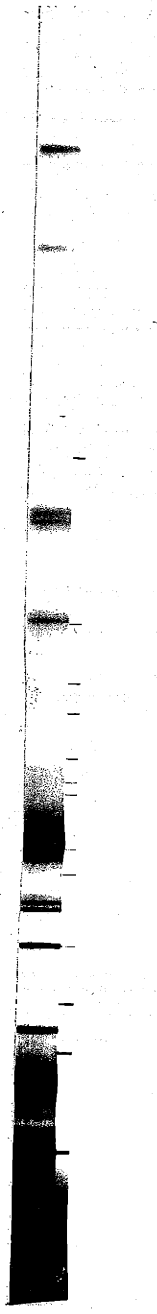
\*However an infrared band has been reported at  $480 \text{ cm}^{-1}$  by Barnes and Haccuria. See Table VII.

Table II - Raman Spectrum of Quartz ( $\text{cm}^{-1}$ )

This research	Saksena <sup>31</sup>	Rasetti <sup>30</sup>	Nedungadi <sup>29</sup>	Krishnan <sup>20</sup>
128	128(13)*	128 (5)	127(20)	39 (1) 95 (2) 145 (3) 170 (2)
206	207(10)	207 (10)	207(15)	206 (14) 240 (2)
265	267(5)	265.9(2)	263(4)	266 (8)
356	358(4)	356.5(3)	354(6)	357 (7)
394	391(3)	394.4(1)	397(4)	394.8(6)
402	403(3)	403.5		403.8(6)
450	452(3)		453(3)	452 (7)
465	466(30)	466.4(20)	465(30)	466 (30)
	479(0)			488
	505(1)		501(1)	509 (4)
				530
				548 (2)
697	695(2)	696.8	694(3)	588 (0)
796	795(2)	796.6(1)	794(3)	696.4(5)
806	806(3)	809.3(2)	805(3)	730
				794.7(6)
				805.8(6)
				842 (1)
				864
				925
				944 (0)
				961
				1040 (0)
1066	1063(1)	1063.1(1)	1064(2)	1063.7(5)
1081	1082(2)	1082.5(2)	1082(2)	1081.9(4)
1160	1160(4)	1160.2(2)	1158(5)	1159.3(8)
1228	1228(1)	1227 (1)	1228(2)	1228.0(4)

\* NUMBERS IN PARENTHESES ARE ESTIMATED INTENSITIES

Optic axis parallel to the direction of observation



Optic axis perpendicular to the direction of observation

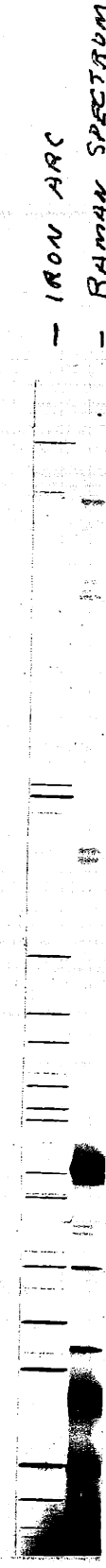


Fig. 1 Raman Spectrum of - Quartz

We have not found all the lines reported by Krishnan who excited the spectrum by Hg 2537A and used long exposure times.

The frequencies of the Raman bands of vitreous silica are given in Table III together with the values taken from the literature. The spectra given by the three samples of vitreous silica employed were identical in all respects. The agreement between our measurements and those reported in the literature is fairly good. However we have found no indication on our densitometer curves of the maxima found by some workers by visual examination in the region 250 to 500  $\text{cm}^{-1}$ . In some cases we have been unable to find very weak lines reported by other workers. However, the early work of Gross and Romanova<sup>12</sup> is rather doubtful as many of their bands have not been reported by other workers. The band at 800  $\text{cm}^{-1}$  has been reported as a doublet by Krishnan<sup>21</sup> but our densitometer curves indicated only a single asymmetric band whose maximum is at 794  $\text{cm}^{-1}$ . Krishnan did not find the band at 599  $\text{cm}^{-1}$  because of interference by the mercury line at 2576A (609  $\text{cm}^{-1}$ ).

The intensities as photographically determined of vitreous silica and quartz are compared in Figure 2. These measurements are based on plates taken under identical conditions with samples of the same size and shape and with exposures of the same duration. After a correction was applied for the difference in density between quartz and vitreous silica (i.e difference in number of  $\text{SiO}_2$  groups per unit volume), the integrated intensities of the two

Table III - Raman Bands of Vitreous Silica in  $\text{cm}^{-1}$

This research	Harrand <sup>15</sup>	Krishnan <sup>21</sup>	Kujumzelli <sup>22,23</sup>	Gross and Romanova <sup>12</sup>	Gross and Kolesova <sup>11</sup>
$\nwarrow 100$	95	$\uparrow 30\text{--}120(\text{vs})$	$\uparrow 230$	$212(\text{fs})$	
$\nwarrow 275$		$\uparrow 285(\text{s})$		$263(\text{fs})$	
$\nwarrow 425_{\text{max}}$		$\uparrow 370(\text{vs})$		$322(\text{s})$	
$\nwarrow 495$		$\uparrow 430(\text{vs})$	$\uparrow 450$	$380(\text{s})$	
$\nwarrow 599$	500	$\uparrow 495(\text{vs})$	500	$445(\text{s})$	$441$
$\nwarrow 730?$	595-612			$500(\text{s})$	$494$
$\nwarrow 793(\text{c})$		$\uparrow 635(\text{vw})$	607	626	601
$\nwarrow 860?$		$\uparrow 775\text{--}805(\text{s})$	720?	$666(\text{w})$	701
$\nwarrow 1060(\text{c})$		$\uparrow 810\text{--}845(\text{fs})$	$780\text{--}840$	$741(\text{vw})$	$791(\text{c})$
$\nwarrow 1180(\text{c})$		$\uparrow 885\text{--}940(\text{vw})$		$800\text{--}834(\text{s})$	
		$\uparrow 910$	915?		
		$\uparrow 1020\text{--}1100$	$1030\text{--}1090$	$1031\text{--}1088$	$1026$
		$\uparrow 1140\text{--}1245(\text{w})$	$1160\text{--}1235$	$1190\text{--}1235$	$1075(\text{c})$
					$1138$
					$1219$
					$1385$
					$1535$

w = weak  
 ? = questionable  
 c = band center

v = very  
 f = fairly  
 s = strong

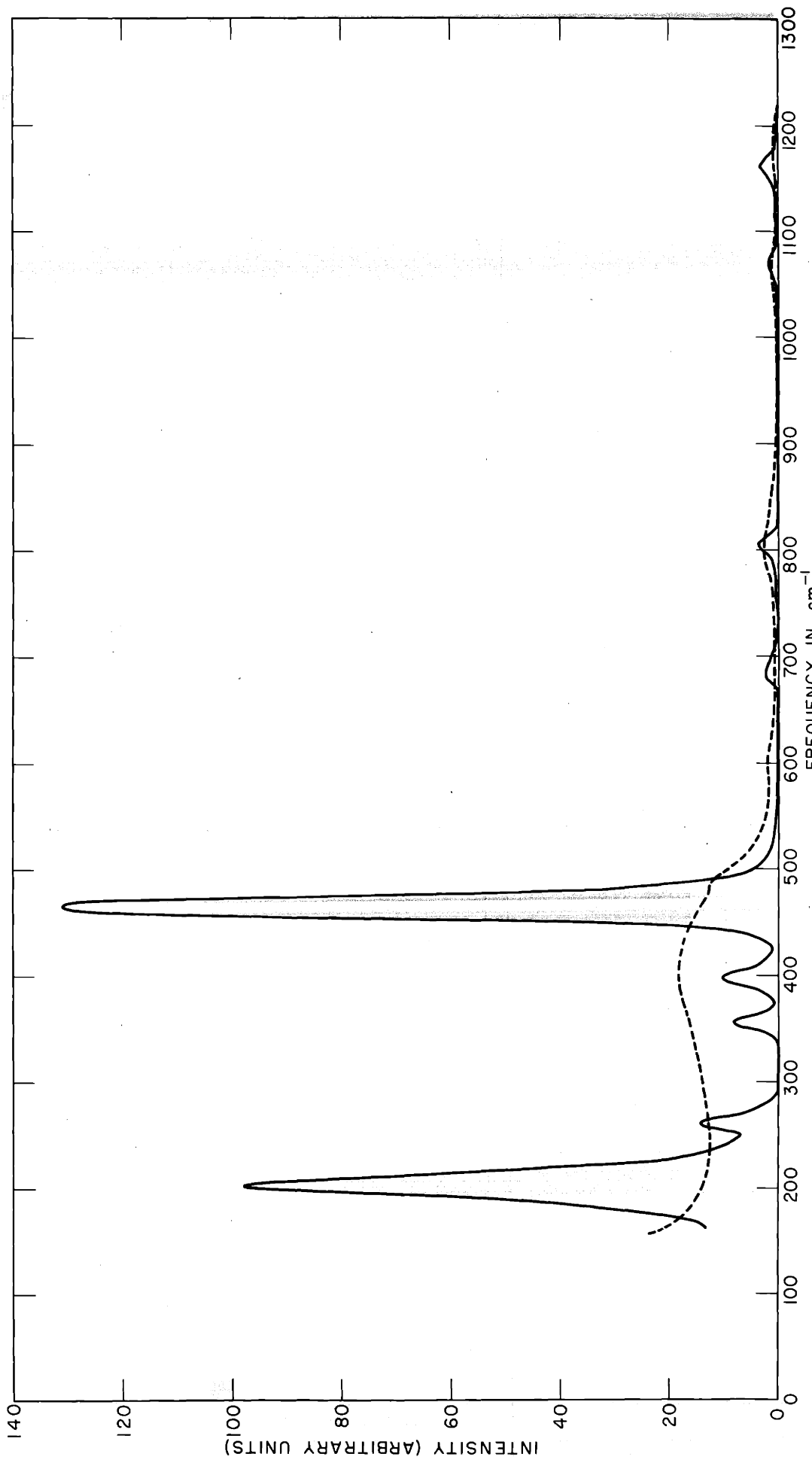


FIG. 2 COMPARISON OF RAMAN INTENSITIES OF QUARTZ AND VITREOUS SILICA

spectra from 160 to 1300  $\text{cm}^{-1}$  were equal within experimental error. However, the inaccuracy of the photographic intensity measurements may be seen by comparing Figure 2 with Figure 3 which shows the Raman spectrum of quartz as recorded photoelectrically. It will be noted that the ratios of the intensities of the 207 and 466  $\text{cm}^{-1}$  lines are quite different in the two figures. The factor-of-ten greater exposure time necessary to photograph the spectrum of vitreous silica as compared to the exposure time necessary in the case of quartz is due only to the broad, diffuse nature of the bands in vitreous silica.

Figure 4 shows the intensities of the Raman bands of vitreous silica and the glasses as a function of frequency. The plates upon which these curves were based were all of seven hours duration and taken under identical conditions, corrections being applied for differences in sample sizes. These spectra were photographed with the grating spectrograph in the second order using a 16  $\text{cm}^{-1}$  spectral slit width. The frequencies of the Raman bands in the glasses are given in Table IV. It is estimated that the precision in measuring the bands is  $\pm 5 \text{ cm}^{-1}$  for those measured from densitometer curves.

No intensity measurements were performed on the glass

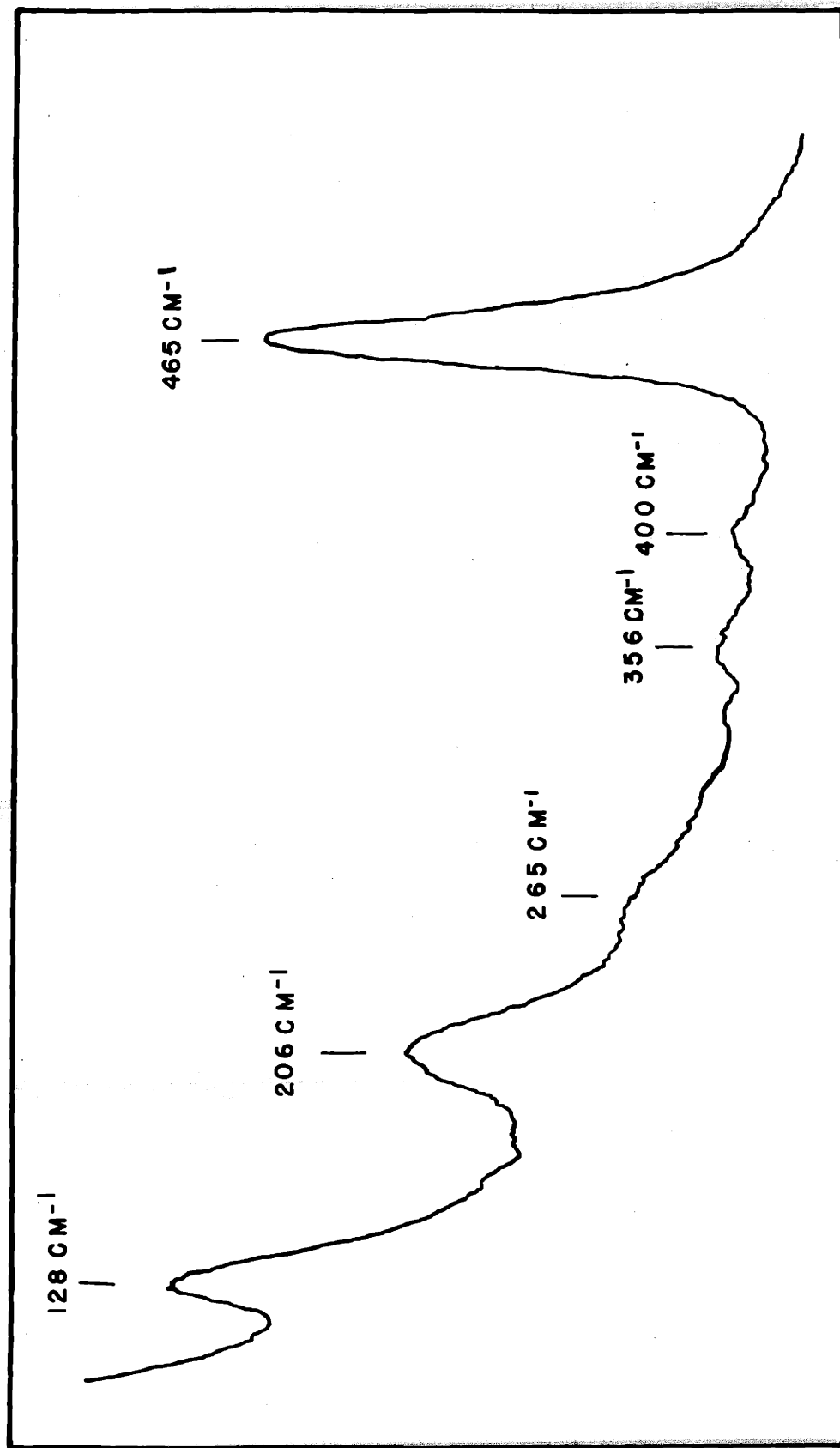


FIG. 3 RAMAN SPECTRUM OF QUARTZ BELOW  $500 \text{ cm}^{-1}$  AS RECORDED  
PHOTOELECTRICALLY

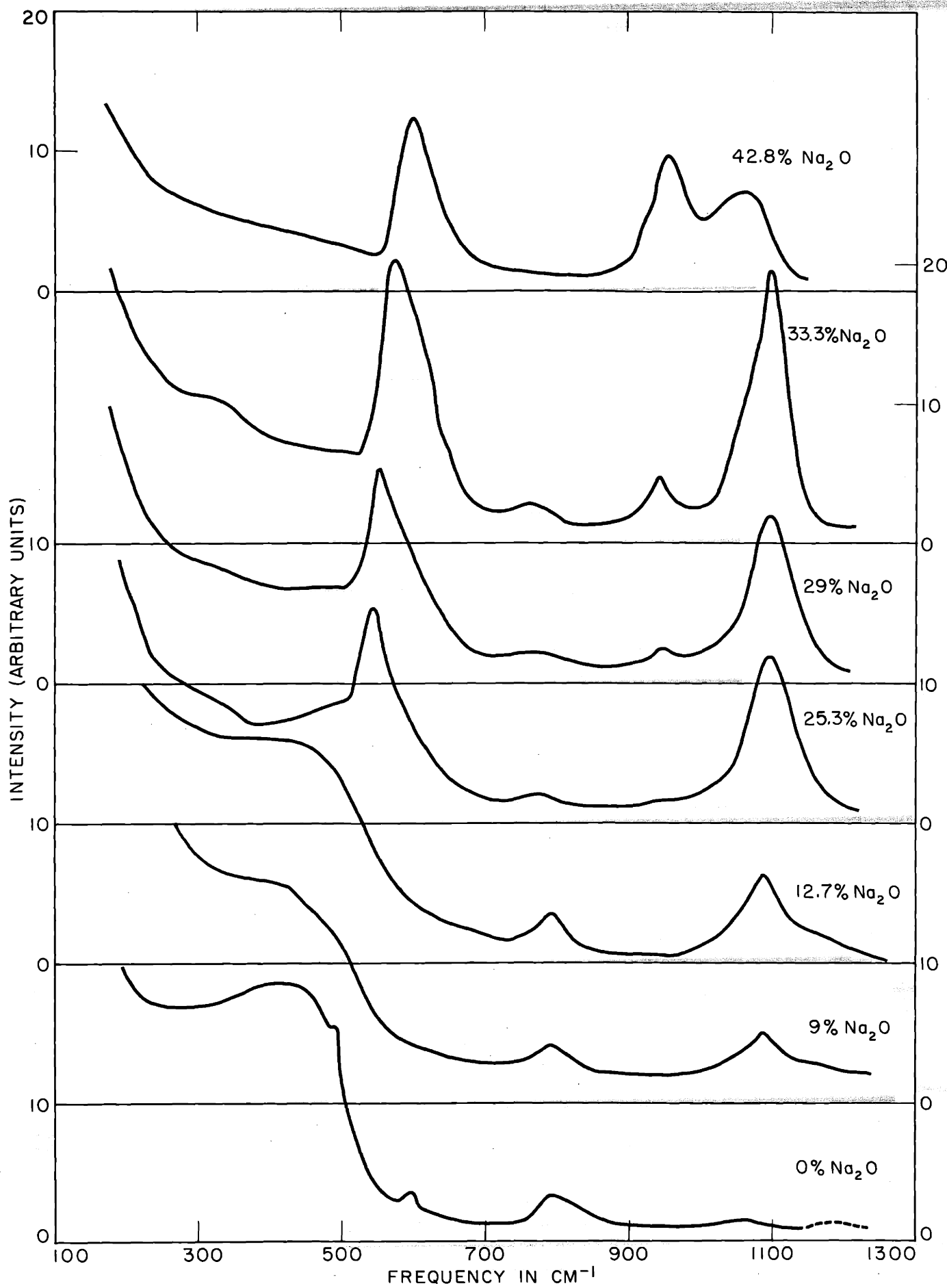


FIG. 4 RAMAN SPECTRA OF THE SODA-SILICA GLASSES

Table IV - Raman Frequencies of Na<sub>2</sub>O-SiO<sub>2</sub> Glasses

Mole % Na <sub>2</sub> O	Frequencies in CM <sup>-1</sup>							
0	**	425	490	599	(720)	794	1060	1180
9.01		440	(512)*	(600)		791	1088	(1170)
12.69		440	(525)	(600)		797	1088	(1170)
16.05		(450)	(522)			(810)		(1095)
25.26		(450)	543			779	947	1098
29.0			551			769	951	1097
33.26			575			757	942	1099
42.82			601		(740) (850)	954	1060	

\* The frequencies in parenthesis have been measured by visual comparison with the iron spectrum.

\*\* The frequencies given in this column are the maxima of the continuum.

of 16.05 mole % Na<sub>2</sub>O since samples of this composition gave spectra with intense background because of their strong Rayleigh or Tyndall scattering of arc continuum. This strong scattering, evidently caused by devitrification, was noticed early in this research and new samples of approximately the same composition were prepared which were annealed only long enough to prevent fracture. When first received, these samples gave spectra with low background, but eight months later, when the intensity measurements were made, they scattered so strongly that study on the grating instrument was not possible because of the intense grating ghosts produced by the exciting line. The Rayleigh scattering of samples 1 and 2 was also high but useful spectra could be taken. The samples 1, 2, and 3 are considered most prone to devitrify.

Comparison of Table IV and Table V, which contains the frequencies of the Raman bands of the soda-silica glasses as reported in the literature, shows reasonably good agreement between both frequencies and qualitative intensities. The bands found by Gross and Kolesova<sup>11</sup> at 600 cm<sup>-1</sup> for all the glasses could be measured for glasses 1 and 2 but appeared on our curves only as an asymmetry of the strong band 540-600 cm<sup>-1</sup> in the spectra of the glasses of higher soda content. The band at 1125-1150 cm<sup>-1</sup> found by the same workers appeared only for glasses 1 and 2 on our curves and could not be detected for glasses of higher soda content.



These workers also reported a band around  $1050\text{ cm}^{-1}$ . There is some indication of this band on our plates but it does not show up on the densitometer curves. Since Vuks and Ioffe also used photometric means to investigate their spectra while Gross and Kolesova's measurements were made by visual means, the frequencies given by the latter workers are open to some doubt as to precision.

From the curves (Figure 4) it can be seen that there exists Raman scattering below  $500\text{ cm}^{-1}$  in the spectra of all glasses, the intensity of the scattering decreasing with increasing soda content. This scattering has not been reported by other workers who investigated only glasses of higher soda content than 20%. It becomes increasingly difficult to distinguish Raman scattering from the Rayleigh scattered background as one approaches the exciting line. Thus, despite the fact that an attempt was made in some cases to subtract the Rayleigh scattering from the spectral curves, it is uncertain just how much of the intensity below  $400\text{ cm}^{-1}$  is due to Raman scattering.

Krishnan has found a Raman band in vitreous silica extending from 30 to  $120\text{ cm}^{-1}$  using Hg2537A as exciting line. Thus it is probable that the glasses also have Raman bands in this region. In the spectral region around 2537A there was no continuum in the mercury arcs used by Krishnan and hence the background in the Raman spectra was very low. However, soda glasses absorb ultra-violet and can not be studied with this mercury line.

One could investigate the low frequency region using Hg 4358A only by employing arcs of very low continuum in the region around 4400A and an effective filter such as praseodymium chloride solution. Other possibilities would be to use different mercury lines in the visible as exciting lines such as Hg 4047A or Hg 5461A where the intensity of the continuum may be somewhat less, or to excite the spectra with He 3889A or some other suitable spectral line. If photoelectric recording of the glasses had proved possible, the intensity of this background could have been subtracted from the recording down to, say 100 cm<sup>-1</sup>, giving reliable results.

Semiquantitative polarization measurements were made on the spectra of vitreous silica and the glasses containing 12.7 and 42.8 mole percent Na<sub>2</sub>O. The results of these measurements are given in Table VI. The depolarization ratios of the Raman lines of carbon tetrachloride as measured under identical conditions are given for comparison. It was not possible to measure the ratios for the weaker bands of vitreous silica and the glasses with the exposure times used.

Comparison with the completely polarized band of CCl<sub>4</sub> shows that any band with a depolarization ratio in the neighborhood of 0.1 is completely polarized. All the bands measured are polarized to some extent.

Table VI - Depolarization Ratios  $\rho$

Composition	Band	$\rho$ (measured)	$\rho$ (actual)
0% Na <sub>2</sub> O	425	strongly polarized	
0% Na <sub>2</sub> O	500	strongly polarized	
	794	.35	
	1060	.65	
12.7% Na <sub>2</sub> O	440	strongly polarized	
12.7% Na <sub>2</sub> O	790	moderately polarized	
	1088	.09	
42.8% Na <sub>2</sub> O	601	.10	
42.8% Na <sub>2</sub> O	954	.10	
	1060	.15	
CCl <sub>4</sub>	218	1.0	.857
CCl <sub>4</sub>	314	1.1	.857
	458	.10	0

Harrand<sup>15</sup> has reported that the bands at 794 and 1060 cm<sup>-1</sup> are depolarized. However it can be seen from the measurements on CCl<sub>4</sub> that the direction of the error in our experiments was such as to make the depolarization ratios observed higher than the actual ratios. Thus any band that we report as polarized cannot be depolarized.

### III. Discussion of Results

#### A. Raman Spectrum and Structure of $\alpha$ -Quartz

##### 1. Classification of Frequencies

Several workers have interpreted the infrared and Raman spectra of quartz, the most complete interpretation being that of Saksena<sup>31</sup> (1940). Since 1940, however, there have been several studies of the infrared spectrum of quartz which have made necessary a new interpretation. The infrared bands of quartz and their polarization characteristics are given in Table VII. These values, comprising both reflection and absorption data, have been taken from the literature.

If vibrational frequencies are measured by infrared reflection methods, calculations need to be carried out to obtain the actual vibrational frequencies from the reflection maxima.<sup>32</sup> Much of the infrared data on quartz in the literature is uncorrected reflection data and thus not reliable. The vibrational frequencies given by Simon and McMahon are based on corrected data and appear reliable.<sup>35</sup> It must also be pointed out that the absorption measurements of very intense infrared bands such as the one at  $1065\text{ cm}^{-1}$  give frequencies which

Table VII - Infrared Frequencies of Quartz in Cm<sup>-1</sup>

Simon <sup>34</sup>	Simon and McMahon <sup>35</sup>	Czerny <sup>9</sup>	Barnes <sup>4</sup>	Liebisch and Rubens <sup>25</sup>	Haccuria <sup>13</sup>	Coblentz <sup>7</sup>
		128 (a)	128 (a)			
		263 (a)	263 (a)	364 (e)		
			385 (a)	385 (o)		
455 (o)				476 (o)	467 (a)	
			488 (a)		481 (a)	
520 (e)				508 (e)	522 (a)	
540 (e)					694 (a)	687 (o)
		780 (e)			775 (a)	
		800 (o)	800 (a)		794 (a)	799 (o)
		1055 (e)				
		1065 (o)			1087 (a)	
		1160 (o)				1190 (a)
		1250 (o)				

a = absorption measurement

o = reflection measurement ordinary ray (class E)

e = reflection measurement extraordinary ray  
(class B)

are not the true vibrational frequencies because of the high reflection near such absorption bands.

From the results of x-ray analysis<sup>48</sup> it is known that quartz belongs to the space group  $D_3^4$  and has three  $\text{SiO}_2$  groups per unit cell. The symmetry of the unit cell is therefore  $D_3$  with a three-fold screw axis ( $C_3$ ) along the optic axis and three two-fold axes ( $C_2$ ) perpendicular to  $C_3$ . The atomic arrangement is spiral around  $C_3$  with the silicon atoms lying on the  $C_2$  axes and the oxygen atoms lying on no element of symmetry. Four oxygen atoms are tetrahedrally arranged about each silicon atom at a distance of 1.61A.

We shall now obtain the selection rules for the infrared and Raman spectra of quartz, using a method based on the symmetry of the unit cell. This method has been described several times in the literature (for example, see Winston and Halford<sup>45</sup> or Hornig<sup>18</sup>). Since there are 9 atoms per unit cell, there are  $3 \times 9 = 27$  vibrational degrees of freedom. There is a general selection rule for crystals<sup>18,39</sup> which states that only those vibrations for which corresponding atoms of neighboring unit cells vibrate in phase can be excited in infrared absorption or in the Raman effect. That is, only those vibrations in the crystal

which have infinite wave length can be active. Thus the three degrees of freedom corresponding to translations of the unit cell as a whole are not active either in infrared absorption or in the Raman effect and we have 24 degrees of freedom to be considered.

To determine how these 24 degrees of freedom are apportioned among the symmetry species of the  $D_3$  symmetry group of the unit cell, we have merely to use the standard group theoretical formulas or consult the tables given by Herzberg<sup>17</sup>. The character table for the  $D_3$  group is given in Table VIII. The number of vibrations in each symmetry species and their infrared and Raman activity are also given here. Whether the vibrations of a given species will be active in infrared absorption or in the Raman effect is determined just as it is in the case of molecules<sup>17</sup>. The analysis (Table VIII) shows that of the 24 genuine vibrational modes of the unit cell, four are in the totally symmetric class A, which is Raman active and infrared inactive, four are in the infrared active, Raman inactive class B, and eight are in the degenerate class E which is both infrared and Raman active.

The Raman lines in class A and class E may be distinguished by study of the polarization characteristics of the Raman lines. This has been done by several workers whose results are in good agreement.<sup>6,31</sup>

Table VIII - Character Table for D<sub>3</sub> Group and Selection  
Rules for Quartz

Class	E	2C <sub>3</sub>	3C <sub>2</sub>	Total No. Modes	Trans- lations	No. Genuine Modes	Selection Rules
A	1	1	1	4	0	4	RA
B	1	1	-1	4	γ	4	IR
E	2	-1	0	9	α, β	8	RA + IR

γ = direction of optic axis

α, β = two perpendicular axes perpendicular to γ

RA = Raman active

IR = Infrared active

The infrared active vibrations of class B are excited only when the electric vector is parallel to the optic axis. That is, these vibrations give rise to a change in dipole moment whose direction is parallel to the optic axis. The vibrations of class E change the dipole moment in a direction perpendicular to the optic axis. The infrared bands of class B and class E are distinguished by studies of the crystal with various orientations in polarized infrared radiation.

The classification of the infrared and Raman bands of quartz based on the preceding reasoning, is given in Table IX. This assignment of the Raman bands agrees in most respects with the ones reported in the literature. An exception is the Raman band at  $452 \text{ cm}^{-1}$  which, previously unclassified, is now assigned as a class E fundamental because of the infrared band found at  $455 \text{ cm}^{-1}$  by Simon. The weak band at  $1228 \text{ cm}^{-1}$  cannot be classified as an overtone or combination band resulting from any of the strong fundamentals. It should also be pointed out that Krishnan<sup>20</sup> has found, in addition to the fundamentals and overtone and combination bands, 12 lines in the region  $0\text{-}1040 \text{ cm}^{-1}$  that cannot be classified.

Reference to Table VII shows that in the region around  $460 \text{ cm}^{-1}$  the agreement among the infrared data of various

Table IX - Classification of the Fundamental Frequencies  
of Quartz

Class	Raman Frequencies	Infrared Frequencies	Mode
A	207 356 466 1082		$Q_{A_1}$ $Q_{A_4}$ $Q_{A_2}$ $Q_{A_3}$
B		365 520 780 1055	$Q_{B_3}$ $Q_{B_2}$ $Q_{B_1}$ $Q_{B_4}$
E	128 265 392 } 403 } 452 695 795 } 807 } 1063 1159	128 263  455 694 800 1065 1160	$Q_{E_{2a}}$ $Q_{E_{6a}}$ $Q_{E_{4a}}$ $Q_{E_{1a}}$ $Q_{E_{3a}}$ $Q_{E_{7a}}$ $Q_{E_{8a}}$ $Q_{E_{5a}}$

workers is poor. According to I. Simon<sup>34</sup>, his corrected frequency at  $455 \text{ cm}^{-1}$  has a precision of  $\pm 10 \text{ cm}^{-1}$  or better and seems to arise from a dipole change perpendicular to the optic axis although the possibility of a component parallel to the optic axis cannot be ruled out. It is on this basis that we have identified it with the class E Raman line at  $452 \text{ cm}^{-1}$ .

The bands at  $385 \text{ cm}^{-1}$  and  $481.8 \text{ cm}^{-1}$  in the infrared spectrum have no counterpart in the Raman spectrum, although at least the first arises from a dipole-moment change perpendicular to the optic axis. Also the Raman doublet at  $397-403 \text{ cm}^{-1}$ , which has been assigned as a class E fundamental has no infrared counterpart.

As Simon<sup>33</sup> has shown, reflection data must be corrected in the strongly reflecting and absorbing region around  $1100 \text{ cm}^{-1}$ . In the classification of the fundamental frequencies (Table IX) the corrected infrared data of Simon and McMahon have been used in the frequency range studied by them. For the three infrared active fundamentals below  $455 \text{ cm}^{-1}$ , those of the references listed in Table VII have been employed.

## 2. The modes of vibration in quartz.

One can scarcely hope to find the normal modes of such a complicated system as the quartz lattice. Thus,

in the correlating of frequencies with vibration modes in quartz, the discussion must of necessity be only approximate and qualitative. Barriol<sup>5</sup>, for example, has considered the possible motions in  $\beta$  -quartz, where visualization of the symmetry modes is simpler because of the higher space-group symmetry ( $D_6^4$ ). Thus, by setting up possible symmetry modes in  $\beta$  -quartz and noting how the six symmetry classes of  $\beta$  -quartz merge to give the three classes of  $\alpha$  -quartz, he was able to discuss the motions of the  $\alpha$  -quartz lattice.

Saksena<sup>31</sup> has given a set of symmetry modes for  $\alpha$  -quartz, An actual normal mode belonging to a given symmetry class can, of course, be expressed as a linear combination of the symmetry modes belonging to the class.

As a first step toward a correlation of frequencies and vibrational modes, one can consider three types of modes in quartz: first, low frequency modes involving primarily the heavy silicon atoms, second, middle frequency modes such as bending modes\*, involving primarily motions of oxygen atoms and third, high frequencies modes involving stretching of the Si-O bonds.

The observed frequencies of quartz show a wide division between the high stretching frequencies and the lower frequencies. There is a separation of  $250 \text{ cm}^{-1}$  between the highest

\*In the remainder of the discussion the middle frequency modes will be referred to, for convenience, as "bending modes". This is not to be taken as a suggestion that the forces involved are necessarily directed valence-bond forces such as exist in  $\text{H}_2\text{O}$ .

bending mode and the lowest stretching mode. On the other hand, as might be expected from the relative weights of the oxygen and silicon atoms, the distinction between the oxygen bending frequencies and the heavy atom frequencies is not sharp. However, some degree of separation is possible.

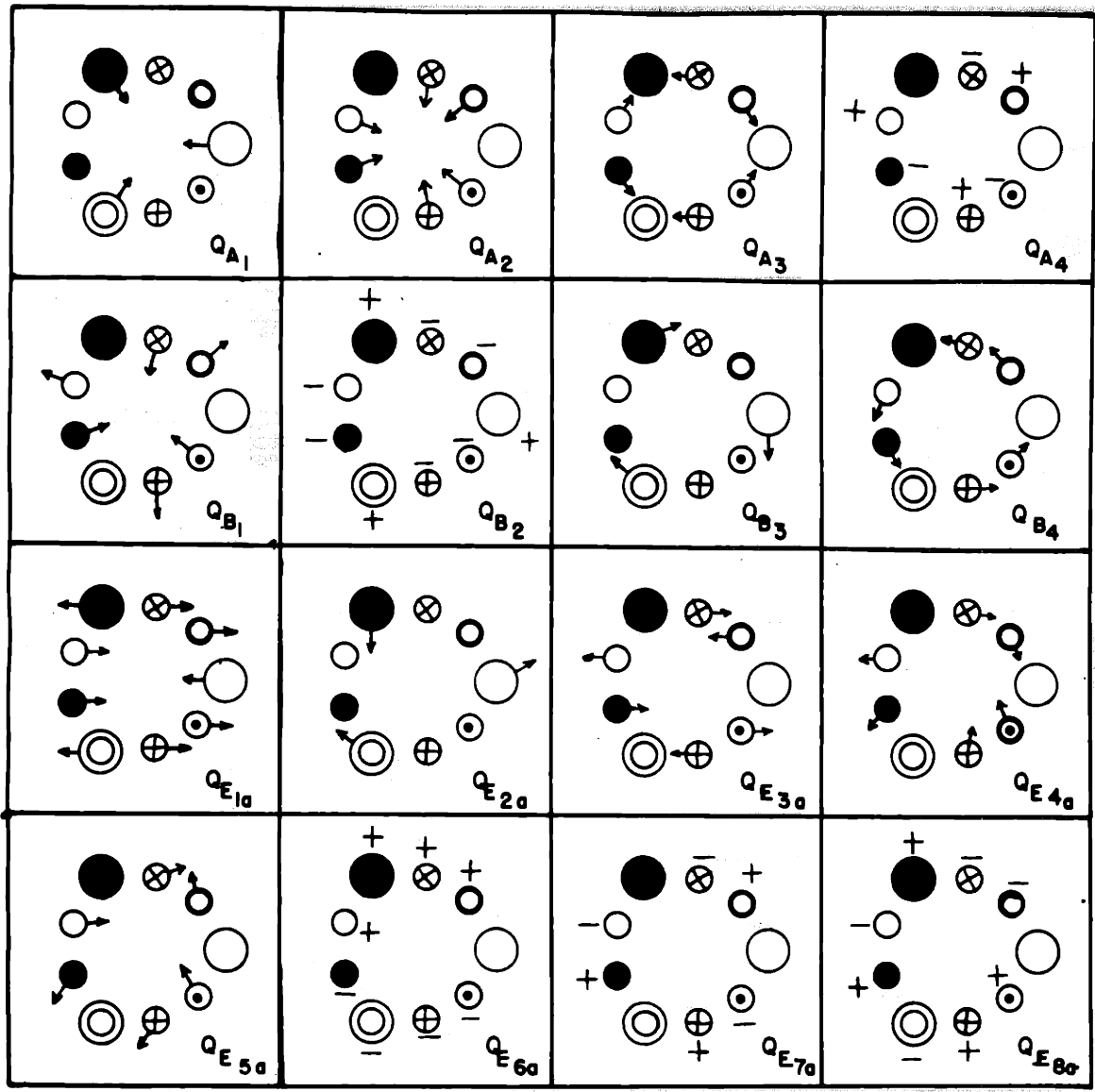
Of the four degrees of freedom of totally symmetric class A, the oxygen atoms contribute three and the silicon atoms one (see, for example, Herzberg<sup>17</sup>, Table 36). Thus the class A mode at 207 cm<sup>-1</sup> is largely a motion of the silicon atoms, while those at 356, 466 and 1082 cm<sup>-1</sup> involve motions of the oxygen atoms, the last being the totally symmetric stretching frequency.

Class B has five degrees of freedom, three contributed by the oxygen atoms and two by the silicon. However, the situation is somewhat complicated by the presence of one translational degree of freedom which, of course, contains motions of both oxygen and silicon atoms. However, we can set up four symmetry modes corresponding to the genuine vibrational degrees of freedom. The first will involve a motion of the silicon atoms only and may be identified with the class B mode at 364 cm<sup>-1</sup>. The second, involving motions of both silicon and oxygen atoms, comes at 520 cm<sup>-1</sup>. The other two class B modes involve only oxygen motions and come

at 780 and  $1055\text{ cm}^{-1}$  the latter being the stretching mode.

There are 18 degrees of freedom occurring in 9 degenerate pairs in class E. Of these 9 pairs, 6 are contributed by the oxygen atoms and 3 by the silicon atoms. One pair is contributed by the two translations perpendicular to the three-fold axis and will contain both oxygen and silicon motions. The vibration at  $128\text{ cm}^{-1}$  doubtless arises motion of the silicon atoms. Perhaps we cannot expect to separate the oxygen motions from the silicon motions in the remaining class E modes except to say that the class E vibration at  $265\text{ cm}^{-1}$  is probably due primarily to motion of the silicon atoms. Of the remaining low and middle frequency modes, most involve motion of the oxygen atoms only. There are two stretching modes in class E, one at  $1159\text{ cm}^{-1}$  and the other at  $1063\text{ cm}^{-1}$ .

The symmetry modes given by Saksena are reproduced in Figure 5 and their correlation with the observed frequencies on the basis of the above discussion given in Table IX. Qualitatively one would expect those modes active in the Raman effect which involve motions of the highly charged silicon ion ( $\text{Si}^{+4}$ ) alone to give rise to intense Raman lines. And, indeed, the frequencies at  $128$  and  $207\text{ cm}^{-1}$  of the modes  $Q_{E_{1g}}$  and  $Q_{A_1}$ , respectively are very intense. Motions of the type  $Q_{A_2}$  are



● ○ ○ SILICONS AT LEVELS 0, 3C/9, 6C/9

○ ○ ○ ● + ⊗ OXYGENS AT LEVELS C/9, 2C/9, 4C/9, 5C/9, 7C/9, 8C/9

FIG. 5 SYMMETRY MODES OF QUARTZ (AFTER SAK SENA)

known to give rise to large changes in polarizability and the line at  $466 \text{ cm}^{-1}$  identified with this mode is the most intense in the entire spectrum.

It must be again emphasized that this discussion serves only as a qualitative guide to the understanding of the spectrum of quartz. Symmetry modes are not normal modes and strictly speaking, cannot be correlated with vibrational frequencies.

B. Raman Spectrum of Vitreous Silica

The structure of vitreous silica according to x-ray analysis<sup>41,42,43</sup> is a disordered one. Each silicon is surrounded by four oxygens at about 1.62A. The O-O distance is about 2.45A, the Si-Si distance 3.2A and the Si-O-Si bond angle about 180°. The relative orientation of one tetrahedral group with respect to a neighboring group around the Si-O-Si bond is random. X-ray analysis gives no definite distances greater than the next-nearest Si-Si distance at 5.2A. Beyond this, the various distances from a given atom to others depend highly on the relative orientations of the  $\text{SiO}_4$  tetrahedra and give rise to no definite maxima in the x-ray pattern.

These data for vitreous silica agree closely with the values for quartz<sup>46,48</sup> for which the Si-O distance is 1.62A, the O-O distance 2.62-2.67A and the Si-O-Si angle 144°. Thus we may expect the same type of binding and the same values of force constants in vitreous silica as in quartz.

From a spectroscopic point of view, the most important difference between quartz and vitreous silica is the lack of order in the latter. The general selection rule for crystals (p. 32) greatly limits the number of modes that can be infrared or Raman active in quartz, with its

regular atomic arrangement. This rule states that only those modes in which corresponding atoms in neighboring unit cells move in phases can be infrared or Raman active. Thus in a crystal containing  $N$  atoms with  $n$  atoms per unit cell, effectively only  $3n-3$  of its  $3N$  normal modes can give rise to infrared or Raman fundamentals. This number may be reduced further by the symmetry of the unit cell. Thus one expects to find a relatively small number of sharp lines in the Raman spectrum of quartz and indeed this is the case.

In vitreous silica, on the other hand, there are no symmetry elements and hence no selection rules that limit the number of active modes. Vitreous silica may be considered to have a unit cell of infinite size with no symmetry. Thus one has a very large number of normal modes to consider. Many modes will give rise to no net dipole moment change or polarizability change over distances comparable to the wave length of light and will make no contribution to the infrared or Raman spectrum. But a large number will make such a contribution and a priori one would expect a large number of frequencies in the spectrum.

In high frequency modes such as the bond stretching type the motions of the two atoms involved are largely

independent of the motions of the rest of the atoms. Thus a mode involving the stretching of the Si-O bond would be expected to have nearly the same frequency in all forms of silica and be nearly independent of the specific nature of the structure. This will also apply to certain types of bending modes which involve only interactions between neighboring atoms.

In contrast, for the low frequency modes involving interactions between large numbers of atoms, the coupling between one region and another in the lattice is high. Thus the number and frequencies of these modes will be highly dependent on the specific nature of the lattice. In particular, in the disordered lattice of vitreous silica, one would expect to find a large number of active modes at low frequencies.

Comparing these predictions with the observed spectrum of vitreous silica (Fig. 2, Table III), we see that in the low frequency region there are a large number of frequencies. In fact, there is a continuum of frequencies from below  $100\text{ cm}^{-1}$  to  $500\text{ cm}^{-1}$ . Because these low frequencies are highly dependent on the specific nature of the lattice, one would not necessarily expect the distribution of spectroscopically active low frequencies in vitreous silica to be closely related to those in the crystalline

forms of silica. Thus in the spectrum of quartz the strongest line is at  $466\text{ cm}^{-1}$ , while in vitreous silica the maximum of the continuum is about  $425\text{ cm}^{-1}$ . However, just as for quartz, the frequencies below approximately  $400\text{ cm}^{-1}$  are due to modes involving chiefly motions of the heavy atoms. For the higher modes, where the forces involved are localized and the coupling is small, one expects fewer discrete frequencies in vitreous silica and a better correspondence between the various forms of silica. Thus the Raman band at  $1060\text{ cm}^{-1}$  in the spectrum of vitreous silica may arise from the same stretching mode as the class E mode in quartz at  $1065\text{ cm}^{-1}$ .

A serious difficulty in the study of the spectra of vitreous materials is the broadness of the bands. This has two effects: the bands are weak and hence difficult to detect and measure; and there is the possibility that even weaker bands may be covered up by stronger broad bands. However the Raman bands at  $1060$  and  $1180\text{ cm}^{-1}$  are symmetric in shape, which indicates that any other bands present are extremely weak and diffuse.

There are two and perhaps three stretching modes in the Raman spectrum of vitreous silica. The two are at  $1060$  and  $1180\text{ cm}^{-1}$  with the possibility that the very weak band at  $910\text{ cm}^{-1}$  is a third stretching frequency. The infrared

spectrum of vitreous silica (Table X) contains three frequencies in the region 900 to 1200  $\text{cm}^{-1}$ , two bands of moderate intensity at 970 and 1152  $\text{cm}^{-1}$  and a very intense band at 1100  $\text{cm}^{-1}$ . None of these occurs near enough to a Raman band to be identified with it if we accept the reported accuracy of the infrared and Raman measurements.

Two bands have been found in this region in the infrared reflection spectrum of cristobalite by Simon and McMahon<sup>35</sup>. The band at 1100  $\text{cm}^{-1}$  is very intense and the one at 1192  $\text{cm}^{-1}$  rather weak. Since neither of these can be related clearly to corresponding bands in the spectrum of quartz, it is evident that even the stretching modes in silica are somewhat dependent on the nature of the lattice.

On the basis of the coincidence between the strong infrared bands in vitreous silica and cristobalite at 1100  $\text{cm}^{-1}$  and 1095  $\text{cm}^{-1}$  respectively, Simon and McMahon<sup>35</sup> have reasoned that the structure of vitreous silica is more nearly like that of cristobalite than that of quartz. They also assume that the band at 1065  $\text{cm}^{-1}$  in quartz is due to a mode of the type that gives rise to the strong infrared band at 1100  $\text{cm}^{-1}$  in vitreous silica. The Raman band at 1060  $\text{cm}^{-1}$  in vitreous silica makes this assumption open to question. In fact, a comparison of the infrared and

Table X - INFRARED SPECTRUM OF VITREOUS SILICA

Simon and  
McMahon<sup>34,35</sup>

Haccuria<sup>13</sup>

465	467
477	
800	794
970	948
1100	1100
1152	1220

Raman spectra of the various forms of silica shows that the stretching frequencies of vitreous silica cannot be uniquely identified with those of some crystalline form of silica.

The lack of coincidences between the Raman and infrared bands is rather puzzling. There might be three reasons for this. First the observed bands because of their broad nature, might hide weaker bands. However, all bands that are strong in the infrared would then have to be weak in the Raman effect, and vice versa. Second, it is possible that certain vibrations could occur in the infrared, for instance, but would be silent in the Raman effect for reasons of symmetry or quasi-symmetry. An example is the strong infrared band at  $1100\text{ cm}^{-1}$  assuming its assignment as a stretching vibration of the type  $\text{Si}-\ddot{\text{O}}-\text{Si}$  is correct.<sup>28,37</sup> If the Si-O-Si bond angle is  $180^\circ$ , then this group effectively has a center of symmetry. Vibrations antisymmetric to a symmetry center are infrared active and Raman inactive<sup>17</sup>. However it seems doubtful that all the lack of coincidences in this region can be ascribed to effects of this sort. A third reason for the lack of coincidences might be inaccurate measurements. This danger applies to both infrared and Raman measurements but especially to the former where both the experimental techniques and the theory are involved.

Just as for quartz, the oxygen bending frequencies in vitreous silica lie in the region from 800 to  $400\text{ cm}^{-1}$ . There are four distinct frequencies in this region (Tables III and X) and in addition, a large part of the continuum in the  $400\text{ cm}^{-1}$  region must be due to modes of this type. These lower bending modes are sure to be more strongly coupled to the heavy atom frequencies than are the higher ones.

The band near  $800\text{ cm}^{-1}$  is remarkable in that it appears in the infrared and Raman spectra of all crystalline forms of silica<sup>13,35</sup> as well as in the spectrum of vitreous silica.

This band is also present in the spectra of the soda-silica glasses up to at least 33.3%  $\text{Na}_2\text{O}$ . Thus while this mode is apparently connected with the structure of the three dimensional network in silica and the silicates, its nature is such that its frequency is independent of the specific symmetry of the lattice.

In summary it can be said that the infrared and Raman frequencies of vitreous silica can be separated into three groups depending on the type of vibration. In the region below  $500\text{ cm}^{-1}$ , the modes become highly dependent on the specific nature of the lattice and the spectrum of the vitreous material is quite different from those of the crystalline forms. Although the frequency distribution in the Raman spectrum of quartz and vitreous silica is different,

no great difference in the total integrated intensity of the Raman scattering is expected. A justification of this expectation is given in the following discussion.

The distribution of frequencies in quartz is different from that of vitreous silica since the atomic arrangements are different in the two substances. As a consequence of the translational symmetry of the quartz lattice, only those normal modes for which the phase angle between corresponding atoms in neighboring unit cells is zero can give rise to infrared or Raman fundamentals (cf. p.32). The intensity of an infrared band\* is proportional to the square of the dipole-moment change produced by the mode of vibration in question. If we let the dipole-moment change associated with a certain vibration of frequency  $\nu$  be  $m_i$  in the  $i^{\text{th}}$  unit cell, the intensity of the infrared absorption will be proportional to

$$\sum_i^N m_i^2$$

where  $N$  are the number of unit cells in a wave length of the radiation of frequency  $\nu$ . However since corresponding atoms in different unit cells vibrate in phase, the dipole-moment changes have the same magnitude, direction and phase. Therefore they are equal and their amplitudes can be added. Thus the intensity will be proportional to

$$N^2 m_i^2$$

The distribution of frequencies in vitreous silica is

\*For ease of visualization, the discussion will be given in terms of dipole-moment changes and infrared intensities rather than in terms of changes in polarizability and Raman intensities. However exactly the same arguments apply to the latter.

different from that in quartz as a consequence of the different atomic arrangements in the two substances. In addition, there is no symmetry and no requirements on the phase angles between neighboring atoms. Thus all the modes are infrared or Raman active. The intensity of an infrared band of frequency  $\nu$  will be determined by the net dipole-component change over a distance of the order of the wave length of radiation of frequency  $\nu$  just as in the case of quartz. The intensity will be proportional to

$$\sum_i^N m_i^2$$

where  $m_i$  is the dipole-moment change associated with a group of atoms of the same size as the unit cell in quartz, there being  $N$  of these groups in the wave length of the radiation. In the case of vitreous silica, however, the  $m_i$ 's in different groups do not have the same phase and the  $m_i$ 's cannot be added, but only their squares. Thus the intensity is proportional to

$$Nm^2$$

where  $m$  is the average dipole-pole moment change in the group of atoms.

Thus in quartz there are only a few sharp bands in the spectra, but they are intense because the dipole-moment change over the wave length of the radiation is large due to the phase relation imposed by the translational symmetry.

In vitreous silica, on the other hand, there are many frequencies in the spectra, but each makes a relatively small contribution since the net dipole-moment changes are small as a consequence of the lack of phase relations between the motions of the atoms.

C. Raman Spectra and Structure of the Soda-silica Glasses

As soda is introduced into the vitreous silica structure, a new kind of bond is formed, in which an oxygen is shared between a silicon and a sodium ion (the Si-O<sup>-</sup> bond). For each sodium ion introduced, an oxygen atom formerly shared by two silicon atoms (the Si-O-Si bond) will now be bonded to only one. Thus, the number of singly bonded oxygens will be equal to the number of sodium ions. Table XI gives the relative number of these as a function of the soda content of the glasses. As the soda content of the glasses is increased, there are increasing numbers of singly bonded oxygens and decreasing numbers of oxygens bonded to two silicones. In the glasses of high soda content the bands corresponding to the motions of the singly bonded oxygens would be expected to be intense. In the glasses of low soda content, a strong resemblance between their spectra and that of vitreous silica would be expected. Figure 4 shows that this is the case. Except for the new band at 1088 cm<sup>-1</sup>, the spectra of the glasses of 9% and 12.7% Na<sub>2</sub>O content are very similar to that of vitreous silica. At 25.3% Na<sub>2</sub>O, two other new bands show up clearly, one at 543 cm<sup>-1</sup> and the other at 947 cm<sup>-1</sup>. These three new bands steadily increase in intensity with increasing soda content up to 33.3% Na<sub>2</sub>O, while the bands related to the spectrum of vitreous silica gradually disappear.

Table XI - The Number and Types of Oxygen Atoms  
Per Silicon Atom in the Soda-silica Glasses

Mole % Na <sub>2</sub> O	Mole % SiO <sub>2</sub>	Si/O	Number of oxygens bonded to two silicon per silicon	Number of singly bonded oxygens per silicon
0	100	.5	4	0
9.0	91	.477	3.0	.2
12.7	87.3	.466	3.7	.3
16	84	.456	3.62	.38
25.3	74.1	.428	3.33	.67
29.0	71.0	.415	3.17	.83
33.3	66.7	.4	3	1
42.8	57.2	.364	2.5	1.5
50	50	.333	2	2

The decrease in intensity of these bands is attributable not only to the decreasing number of moles of  $\text{SiO}_2$  per unit volume (Table I, p. 7) but also to increasing numbers of  $\text{Si}-\text{O}^-$  bonds formed as the soda content increases. Further increase in soda to 42.8% shows a pronounced change in the spectrum in the region around  $1000 \text{ cm}^{-1}$ .

Stretching Frequencies: Just as for vitreous silica we can divide the frequencies into stretching, bending, and heavy-atom frequencies which come in the regions  $1200$  to  $900 \text{ cm}^{-1}$ ,  $900$  to  $400 \text{ cm}^{-1}$ , and  $400$  to  $0 \text{ cm}^{-1}$  respectively. In the stretching region, there will be two types of modes, those involving oxygens bonded to only one silicon and those involving oxygens bonded to two silicons. The stretching frequencies in the Raman spectrum of vitreous silica are weak and are soon submerged by the intense frequencies associated with the singly bonded oxygens as soda is added. However the band at  $1180 \text{ cm}^{-1}$  is evident up to at least 12.7%  $\text{Na}_2\text{O}$  (Figure 4) and possibly up to 40%  $\text{Na}_2\text{O}$  (Gross and Kolesova, Table V). The band at  $1060 \text{ cm}^{-1}$  is close to the strong band at  $1095 \text{ cm}^{-1}$  in the glasses but there is evidence of it up to 33.3%  $\text{Na}_2\text{O}$ .

The stretching frequencies of the singly bonded oxygen are evidently those at  $950$  and  $1095 \text{ cm}^{-1}$ . It is to be noticed, however, that the intensities of these two bands do not vary in the same manner with increasing soda content.

The band at  $1088 - 1100 \text{ cm}^{-1}$  is apparent in the spectra of glasses of very low soda content, and increases in intensity up to 33.3%  $\text{Na}_2\text{O}$ . At higher soda content, it shifts in frequency and decreases in intensity. The band at  $950 \text{ cm}^{-1}$  is not evident in the spectra of the glasses below 25%  $\text{Na}_2\text{O}$ , but from 25%  $\text{Na}_2\text{O}$  increases steadily in intensity up to 42.8%  $\text{Na}_2\text{O}$ .

This difference in behavior suggests the following explanation. We assume that the singly bonded oxygens are randomly distributed among the silicon atoms and ask how many silicon atoms have no singly bonded oxygens, how many have one and how many have two. While the problem of finding the distribution of singly bonded oxygens among the silicones is a function of soda content is very complex, a qualitative discussion will suffice for our purposes.

In the glasses of low soda content, there will be very few silicones with two singly bonded oxygens as compared to those with only one. At 33.3%  $\text{Na}_2\text{O}$  there are about as many singly bonded oxygens as there are silicon atoms (Table XI). This composition will have the highest number of silicones with only one such oxygen, but above 33.3%  $\text{Na}_2\text{O}$  the number of these silicones will decrease while the number having two singly bonded oxygen atoms will rapidly increase. At 50%  $\text{Na}_2\text{O}$  there are, of course, twice as many singly bonded oxygens as there are silicon atoms and each silicon will have, on the average, two such oxygens.

On the basis of this rough reasoning and the behavior of the intensities of the two bands as a function of soda content, the band at  $1095 \text{ cm}^{-1}$  is assigned as a stretching vibration of the  $\text{Si}-\text{O}^-$  bond when there is only one such oxygen per silicon atom. The band at  $950 \text{ cm}^{-1}$  is assigned as a stretching vibration involving the  $\text{Si}-\text{O}^-$  group.

Considered as an isolated unit, this group has two stretching modes,  $\text{Si}-\text{O}_-$  and  $\text{Si}-\text{O}_-$ . The first should be strong in the Raman effect, while the second ought to be weaker and of somewhat higher frequency. The modes involving the  $\text{Si}-\text{O}$ -bond are not strongly coupled with the stretching modes of the silica network and the two modes of the  $\text{Si}-\text{O}_-$  group might be expected to give rise to two Raman frequencies. Under this interpretation the frequency observed at  $950 \text{ cm}^{-1}$  would be due to the symmetric mode. The higher frequency of the antisymmetric mode is probably obscured by the strong band at  $1095 \text{ cm}^{-1}$ . The presence of this antisymmetric mode might explain the shift of the center of gravity of the  $\text{Si}-\text{O}^-$  band from  $1099 \text{ cm}^{-1}$  in the 33.3%  $\text{Na}_2\text{O}$  glass to  $1060 \text{ cm}^{-1}$  in the 42.8%  $\text{Na}_2\text{O}$  glass.

Bending frequencies: The bending frequencies of the oxygen atoms at  $795 \text{ cm}^{-1}$  and in the region 400 to  $500 \text{ cm}^{-1}$  are of the same type as those observed in the spectrum of vitreous silica and greatly decrease in intensity as the soda content increases until they are hardly evident in the glass

of 42.8%  $\text{Na}_2\text{O}$ . The new bending frequencies of the singly bonded oxygen atoms come in the region  $500\text{-}700 \text{ cm}^{-1}$ . Below 25%  $\text{Na}_2\text{O}$ , they are barely detected, but in the glasses from 25 to 42.8%, there is a relatively strong band centered at about  $550 \text{ cm}^{-1}$  which increases in intensity up to 33%  $\text{Na}_2\text{O}$ , after which there is a slight decrease. The asymmetric nature of this band indicates that at least two of these modes contribute to the Raman spectrum. While no intensity measurements could be made on the individual components of the band, the component of lower frequency is by far the more intense. From its intensity at 25%  $\text{Na}_2\text{O}$ , it seems that this component must be due to a bending mode involving the  $\text{SiO}^-$  group.

As one might expect, the bending modes of the  $\text{Si-O}^-$  and the  $\text{Si}$  groups are not strongly coupled to other motions of the lattice, and give sharper bands than the bending modes of the oxygens shared by two silicons. Heavy atom frequencies: The frequencies of the modes involving primarily the motions of the silicon atoms appear below  $400 \text{ cm}^{-1}$  and are difficult to distinguish from the scattered background in the intensity curves. Motion due to the sodium ions, because of the weak binding between the sodium and oxygen ions, also give rise to very low frequencies which cannot be distinguished from the low frequencies of the silicon atoms. In their study of the binary glasses  $\text{Li}_2\text{O-SiO}_2$ ,  $\text{Na}_2\text{O-SiO}_2$ , and  $\text{K}_2\text{O-SiO}_2$ , Gross and Kolesova<sup>11</sup> showed that the spectra are little affected by the nature of the cation. Thus the cation frequencies

are indeed low, and are probably weak and diffuse besides.

Discussion of the results in the literature: In their study of the Raman spectra of glasses, Gross and Kolesova<sup>11</sup> state that there are not bands in the spectra of the soda-silica glasses of less than 45% Na<sub>2</sub>O that cannot be identified with some band in the spectrum of vitreous silica. Thus the strong band in the region 1080-1100 cm<sup>-1</sup> was identified with the band at 1060 cm<sup>-1</sup> in vitreous silica, the band at 950 cm<sup>-1</sup> with the very weak band at 910 cm<sup>-1</sup> in vitreous silica and so on for the lower bands.

If we accept their interpretation of the spectra of the glasses, it is difficult to explain the remarkable changes in intensity and frequency that occur with increasing soda content. One would have to explain why the 490 cm<sup>-1</sup> band in vitreous silica decreases in intensity in glasses of 9 and 12.7% Na<sub>2</sub>O and then increases so markedly with soda content in the glasses of higher soda content. These workers made no intensity measurements nor did they study the low soda glasses. Thus they were unable to follow changes in frequency and intensity step by step. There seems to be no doubt that the new bands that occur in the soda glasses are due to new bonds formed by the introduction of soda.

The infrared frequencies of the soda-silica glasses as

reported by Simon and McMahon<sup>34,36</sup> are given in Table XII. Their curves show a steady decrease in intensity with increasing soda for all bands. An exception is the band in the region  $925-950 \text{ cm}^{-1}$  in the spectra of the glasses of 36%  $\text{Na}_2\text{O}$  and higher. These workers did not find this band in the infrared spectra of the glasses below 36%  $\text{Na}_2\text{O}$ . From this fact they conclude that there exists a definite critical region in the composition at 33%  $\text{Na}_2\text{O}$ . If this band is the same as the Raman band at  $950 \text{ cm}^{-1}$ , as it probably is, then this view is not correct, since the Raman band is evident at 25%  $\text{Na}_2\text{O}$  and increases uniformly in intensity up to 42.8%  $\text{Na}_2\text{O}$ .

The strong infrared band at  $1100 \text{ cm}^{-1}$  decreases both in frequency and intensity with increasing soda. This behavior seems to indicate that this band is not the same as the Raman band in the same region. In addition the frequencies of the two bands do not agree. The explanation of this band as an antisymmetric Si-O-Si vibration agrees with its infrared behavior and its absence from the Raman spectrum.

In the region 450 to  $550 \text{ cm}^{-1}$ , the strong infrared band in the spectrum of vitreous silica increases in frequency and decreases in intensity with increasing soda content. It can be ascribed to one of the bending modes involving the motions of oxygen atoms that are shared by two silicon atoms. This band is the only infrared band in the

**Table XII - Infrared Frequencies of the  $\text{Na}_2\text{O} - \text{SiO}_2$  Glasses.** (Simon and McMahon<sup>34,36</sup>)

Mole % $\text{Na}_2\text{O}$	Frequencies in $\text{Cm}^{-1}$					
0	465	800	970	1100	1152	1360
9	476		(1000)	1100	(1150)	1330
12.7*				1100	(1150)	
16	480 (511)**(530)			1090	(1150)	
23*			(1000)	1087		(1185)
29***	506					
31*				1060		
36*			951	1050		
42.3	514		925	1045		
46*			930	1055		

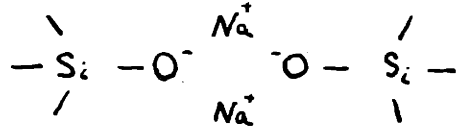
\* These glasses were not measured below  $700\text{cm}^{-1}$

\*\* The bands in parentheses appear as shoulders on the stronger bands

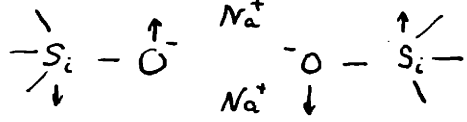
\*\*\* Not measured above  $600\text{ cm}^{-1}$

region 400 to 600  $\text{cm}^{-1}$ .

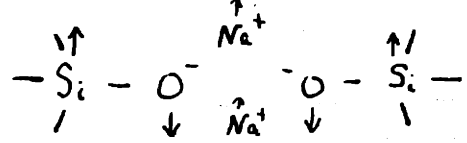
It is puzzling that the bending frequencies of the Si-O<sup>-</sup> group do not appear in the infrared spectra. A possible explanation of this fact is that the sodium ions and hence the singly bonded oxygens might occur in pairs. One would expect that an O<sup>-</sup> ion would try to surround itself with as many Na<sup>+</sup> ions as possible, and this method is a possible way to satisfy this condition. There would then be groups of the type



This configuration has, in effect, a center of symmetry, so that vibrations of the type



are Raman active but infrared inactive, while vibrations of the type



are infrared active and Raman inactive. The frequency of the latter could be lower than that of the former and thus might lie below the range of the infrared measurements, i.e. below 400  $\text{cm}^{-1}$ .

IV. Summary of Structural Conclusions about Silica and  
the Soda-silica Glasses from Infrared and Raman Spectra --  
Suggestions for Future Work.

The infrared and Raman spectra of  $\alpha$  -quartz can be satisfactorily interpreted in terms of the structure as determined by x-ray analysis. However, the success of this interpretation cannot be said to prove that

-quartz has the symmetry of space group  $D_3^4$ . Merely on the basis of the spectra it can be said that quartz has a rather high symmetry, but has no center of symmetry since there are infrared and Raman coincidences in the spectra. The data most easily fit the symmetry of the  $D_3^4$  space group.

The spectra of vitreous silica are not inconsistent with the random network theory of the glassy state<sup>42,49</sup>. In particular the distribution of low frequencies and the broadness of even the higher Raman bands are most easily understood on the basis of the random network theory. Insofar as sharp lines are not found in the Raman spectrum, no support has been found for the view of Babcock et al<sup>2</sup> that there exists a well defined ionic arrangement in vitreous silica. Since these workers have proposed two coexisting structures in vitreous silica, the relative proportions of which are temperature dependent, it is obvious that a study of the Raman spectrum of vitreous silica as at various temperatures should be carried out to test this proposal.

the Raman spectra for any critical region in composition where the structure changes sharply. There is a lack of agreement between the infrared reflection spectra and the Raman spectra which is difficult to understand although some explanations are proposed.

It would be desirable to study the spectra of samples of about 19 and 38 mole percent soda to establish more clearly the changes produced by changing soda content.

It is also suggested that the spectra of other simple silicate glasses be studied. The spectra of the CaO-SiO<sub>2</sub> glasses might help decide whether the Na<sup>+</sup> ions occur in the soda glasses in pairs as the spectra might be interpreted to indicate. For the CaO-SiO<sub>2</sub> system the cations, being divalent, would not be expected to occur in pairs.

## Appendix I - Design, Operation and Performance of the Excitation Unit

### A. Design and Operation

Direct current arcs with water-cooled electrodes have highly desirable characteristics for the excitation of Raman spectra<sup>47</sup>. Because of the low pressure of mercury vapor due to the water cooling, the mercury lines are narrow and the continuum in the region around 4500 Å is very low in intensity. Since this continuum is produced in large part by fluorescence of mercury molecules Hg<sub>2</sub> excited by the 2537 Å mercury line, its intensity is understandably reduced by a decrease in the mercury pressure in the lamp.

Because the temperature is low, the three mercury lines at 4047, 4358 and 5416 Å are very intense relative to the rest of the mercury spectrum in the visible. These three lines are due to transitions from low lying levels in the mercury atom. The two mercury lines at 4339 Å and 4347 Å originate from higher levels and are much weaker in this type of arc. In older types these lines have frequently complicated the Raman spectrum excited by 4358 Å by exciting the stronger Raman lines themselves. Also the mercury lines around 5000 Å which interfere with high-frequency Raman lines are absent in the low pressure arcs.

A further advantage is the absence of foreign gases and oxide-coated electrodes usually present in A.C. arcs for starting purposes. The materials of these electrodes frequently contribute to the spectrum of the A.C. arc in the Raman region around 4500 Å. Recently, Crawford, Welsh, and Harrold<sup>8</sup> have shown that cooling of the arc stream itself results in a further improvement in the spectral characteristics of these arcs.

Since the glasses studied scatter the light of the arcs rather strongly, it seemed desirable to build arcs of this type to decrease the intensity of the interfering continuum. It was decided to build arcs with water-cooled arc streams as well as water-cooled electrodes to utilize most fully the advantages of this type of arc. The first designs tried were built with one cooling chamber for the column and the lower electrode, and a "cold finger" to cool the upper electrode. While this design was fairly successful when the lower electrode was the cathode, the upper electrode was insufficiently cooled and mercury condensed on the walls of the center portion of the arc obscuring the radiation.

The second attempt used a design employed by Stoicheff<sup>38</sup> and proved to be successful. Figure 6 shows the design of the arc. The electrodes are kept cool by water flowing through external chambers. To prevent the condensation

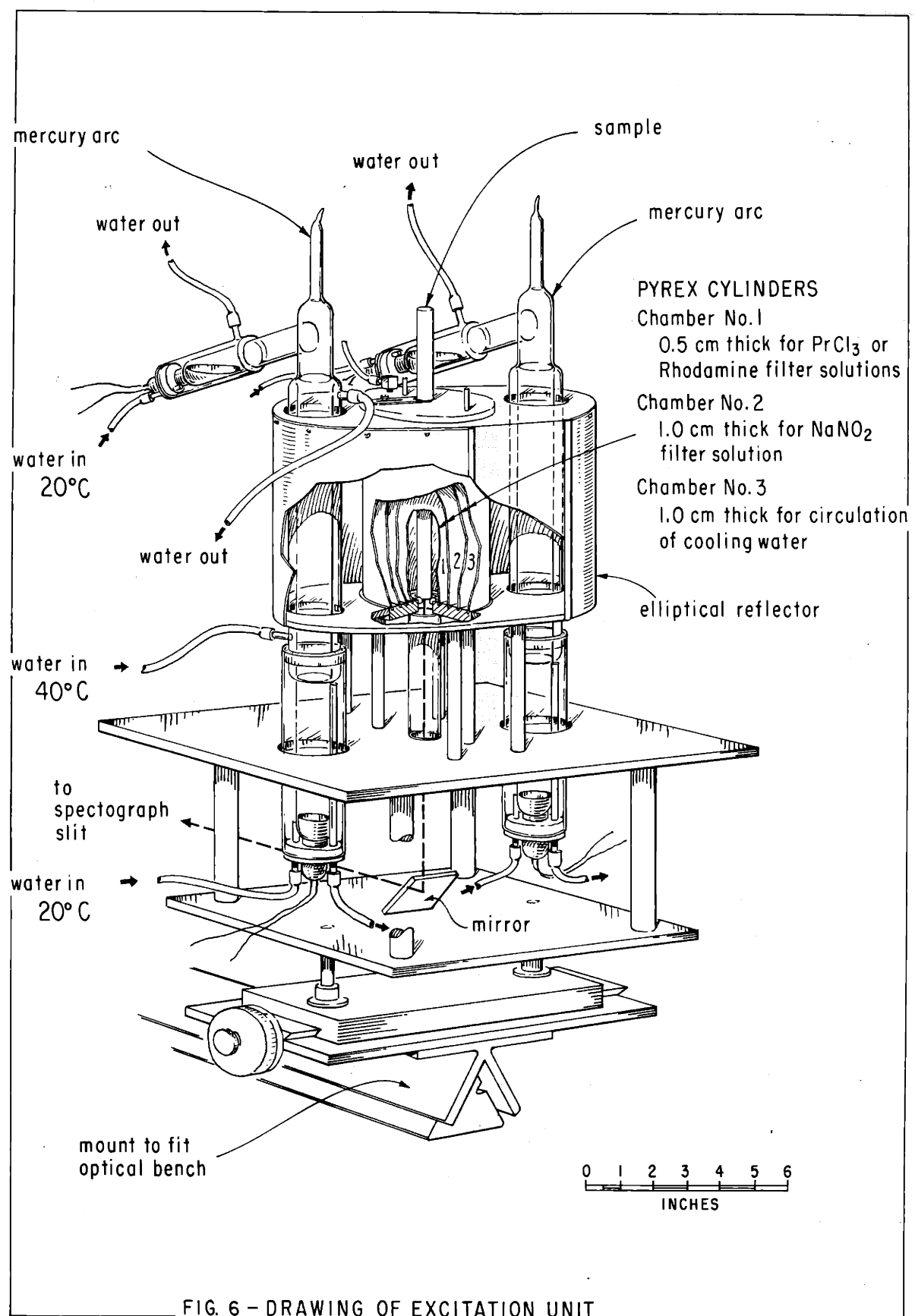


FIG. 6 - DRAWING OF EXCITATION UNIT

of mercury vapor, the arc column is maintained at a higher temperature by circulating hot water through the central jacket. The lamps are made of Pyrex and employ either tungsten or Kovar to lead the current into the mercury pools. The two electrode-cooling jackets are merely glass tubes attached to the arcs by rubber stoppers and cork gaskets.

Figure 6 also shows the unit which was designed to hold two such arcs. It was provided with elliptical reflectors rather than the diffuse reflectors employing a highly reflecting powder like MgO because it might be desirable to make precise depolarization measurements.

For such measurements the sample must be illuminated from one side only with light perpendicular to the direction of observation. These conditions can be more easily fulfilled with specular than with diffuse reflectors.

However, should it become desirable, the reflectors could easily be smoked with MgO. Surrounding the Raman tube, there are chambers formed by concentric Pyrex tubes sealed to brass end plates. These chambers serve for the circulation of cooling water and for filter solutions.

The two arcs were run in series. The circuit is shown in Figure 7. The arcs were started as follows: Water at 40°C was circulated through the center jacket. Each arc was separately started and allowed to warm up before they were started together. After they had warmed

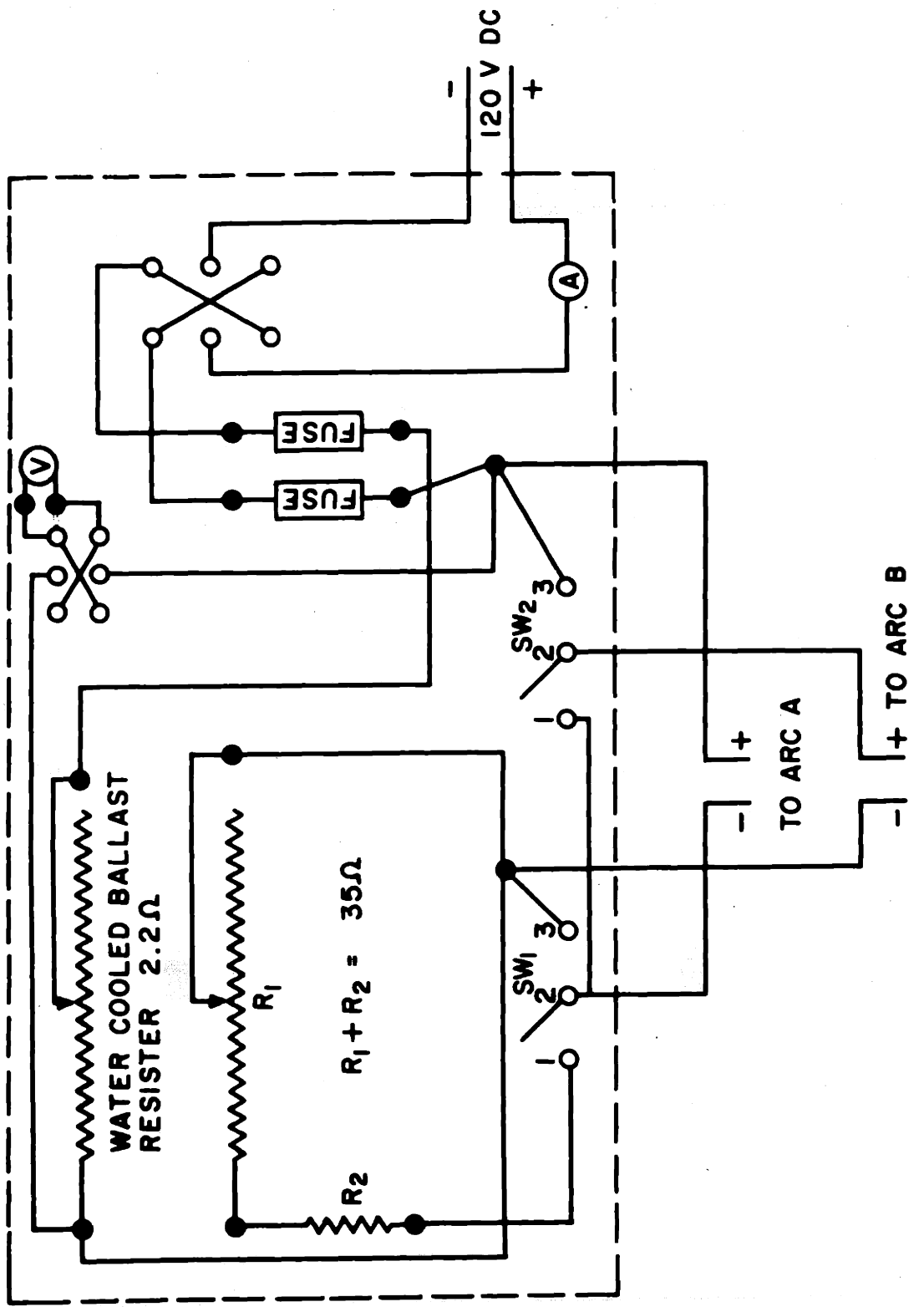


FIG. 7 CIRCUIT DIAGRAM FOR MERCURY ARC POWER SUPPLY

up, switches 1 and 2 (Figure 7) were moved to position 1, thus putting  $R_1$  and  $R_2$  in series with arc A and in parallel with arc B. Arc A was then started. The resistors  $R_1$  and  $R_2$  produce a voltage across arc B and it can then be started.

The actual starting of an arc is accomplished by contacting a leak testing coil to aluminum foil wrapped about the arc at the cathode. The method, used by Stoicheff, is very effective, the arcs starting each time without the necessity of warming the electrodes. In practice the arcs were run at 14.5 amps. At this current the potential drop across the two arcs in series was about 80 volts. However, the voltage was practically independent of the current over a wide range. The tap water used to cool the electrodes emerged at about 30°C. Water at 40°C was circulated through the center jacket and discharged at 60°C.

#### B. Performance

Since the primary advantage of the water-cooled mercury arcs lies in their high ratio of Hg 4358 Å to continuum, the continuum in the old commercial AH-2 arcs and the water-cooled arcs was measured and compared. For the same intensity of Hg 4358 Å, the intensity of the continuum in the water cooled arcs is about 12% of that in the AH-2 arcs. This means that much weaker Raman lines can be detected with the new excitation unit or by

not using optical filters to purify the radiation, exposure times can be reduced as compared to those of the AH-2 source without decreasing the "signal-to-noise" ratio. The reduction in exposure time is particularly important in the study of glass spectra. It is often necessary to use a praseodymium chloride solution with the AH-2 arcs, and this filter transmits only 20 - 25% at 4358 Å in optimum concentration.

At present the intensity of the new excitation unit is about 70% that of the old AH-2 arc unit. When this unit was new, its intensity was about 20% greater than that of the AH-2 arc unit. This fact illustrates one disadvantage of the low pressure D.C. arc. The glass gradually darkens with use and cuts down the light transmitted. At present, after running about 500 hours, the source has about 60% of its original intensity. The blackening can be minimized, according to Stoicheff<sup>38</sup>, by using Corning No. 1720 glass instead of Pyrex in the construction of the arcs.

The new source gives narrower mercury lines than the AH-2 arcs. A comparison of the two sources in this respect is given in Figure 8. This shows the fine structure of the totally symmetric Raman lines of carbon tetrachloride as excited by the two types of arcs. The separation of the two strongest lines is  $3.2 \text{ cm}^{-1}$ .

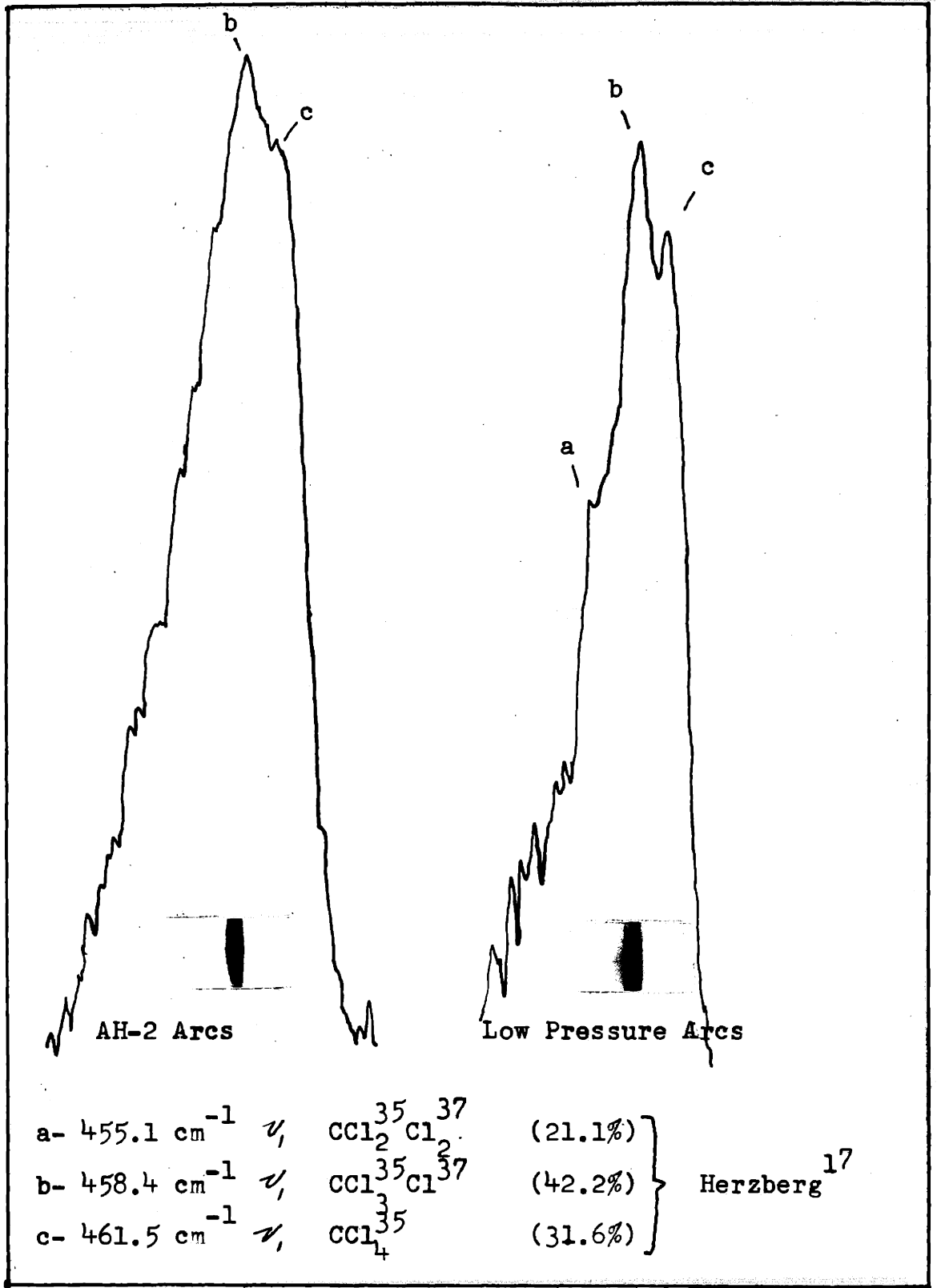


Fig. 8 Fine Structure of the Totally Symmetric Vibration  $\nu$ ,  
of  $\text{CCl}_4$  - Spectrograms and Densitometer Curves for  
AH-2 and Low Pressure Arcs

A further advantage of the new type of arcs is that the intensity of the exciting line is directly proportional to the current. The relation between intensity and temperature of the electrodes has been determined by Kamp, Jones and Durkee<sup>19</sup>. Thus by noting the current and exit temperature of the cooling water at frequent intervals during an exposure, one can keep these quantities constant by suitable adjustment or can take account of the effect of their variation on the intensity. It is estimated that the intensity of the arcs could be maintained constant to within 4% over some months of operation, apart from the slow decrease of intensity associated with the darkening of the glass.

With the AH-2 excitation unit there is no precise way to maintain constant intensity or to estimate the variation in intensity. The intensity of the AH-2 arc varies with temperature and age. During use the arc loses mercury by absorption in the glass envelope and thus the discharge becomes weaker, the temperature lower and the ratio of exciting-line to continuum intensity higher.

## Appendix II - Details of Intensity Measurements

Conditions were kept as constant as possible during each series of exposures and in those cases where conditions could not be the same from one glass to another, appropriate corrections were made. The arc current was kept constant to  $\pm 0.2$  amp by manual adjustment of a rheostat. The temperature of the electrode cooling water was kept constant to  $\pm 3^\circ\text{C}$  while the temperature of the arc column cooling water was kept constant to  $\pm 5^\circ\text{C}$ . The effect of variation in these quantities on the intensity of the exciting mercury line is mentioned in Appendix I. It is estimated that the intensity of the arcs could be maintained constant to 4%.

Accurate, reproducible alignment of the samples in the excitation unit was insured by the design of the unit (see Figure 6, Appendix I). The bottom of the sample is centered by a conical ring. The scattered light from the sample passes out through a hole in this ring and the diameter of this hole determines how much of the cross-sectional area of the sample is seen by the spectrograph. In all experiments this hole was small enough so that the intensity of the spectrum was independent of the diameter of the sample within the range of diameters of the various samples studied.

To correct for the effect of different sample lengths, the variation of the intensity of the Raman spectrum of carbon tetrachloride with length of sample exposed to the arcs was measured photoelectrically. The intensities of

the Raman spectra of the glasses were corrected accordingly.

Because illumination of different portions of the slit did not fill the optics of the spectrograph uniformly, the usual method of plate calibration by means of a step sector at the slit was not followed. Instead the intensity of calibrating light was varied by the inverse-square-law method<sup>16</sup>. The intensity of radiation from a point source falling on the slit is accurately proportional to the inverse square of the distance between source and a diffusing screen used as a secondary source.

The source used in these experiments was a 32 C.P. 6-8 volt auto headlight lamp run from a Cenco constant-voltage transformer at 6.4 volts. The advantages of an incandescent tungsten source of this type are several. The small size of the filament relative to the screen permitted a wide range of intensities without inconveniently long distances from source to screen. A source having a continuous spectrum is a closer approximation to the spectra of the glasses than one with discrete lines. Thus any errors arising from the Eberhard effect are smaller. Finally the intensity of such a source is constant provided a well-regulated power supply is used.

The auto bulb was mounted on an 1 1/2 meter optical bench. The light diffused by the screen was then reflected onto the slit by a right-angle prism. Stray light is a possible danger with this type of arrangement and all

calibration exposures were made with the room lights extinguished. A check with the photoelectric detector showed that stray light was effectively eliminated, since the inverse square law held to the limit of reproducibility of the measurements (about 2%). With this calibration arrangement, eight one-minute exposures were put on each plate. An intensity range of 1 to 64 was obtained with the distances used for the eight exposures.

In order to compare intensities at different wave lengths, it was necessary to know the energy radiated by the source as a function of wave length. This was calculated from Wien's<sup>17</sup> radiation equation using a color temperature of 2905°K. A check with the photoelectric spectrometer agreed quite well with the results of the calculation after corrections were made for the change of dispersion with wave length and the variation of photomultiplier tube response with wave length.

The iron arc spectrum was put on each plate for wave length calibration. The plates were developed for three minutes in D-19 developer, the emulsion being continuously brushed during the process. The plates were then washed 30 seconds in dilute acetic acid (Kodak Stop Bath No. 1), fixed and finally washed for one hour in a supply of constantly changing filtered water.

The densities of the plates were read on a Jarrell-Ash Recording Microphotometer No. JA-2305. This densitometer also serves as a comparator and marks corresponding to the position of the iron lines can be put on the record. Thus frequencies as well as densities can be determined. The densities of the calibration spectra were read at three points,  $100, 700$  and  $1200 \text{ cm}^{-1}$ . These densities were plotted as a function of log intensity and the densities of the Raman bands converted into intensities by interpolation between the curves. A typical set of curves is given in Figure 9. After the intensities of the Raman spectra were read, corrections were made for variations in sample length for the variation of intensity of the calibrating source with wave length.

Since the exposure times of the calibration spectra were one minute and those of the Raman spectra seven hours, the reciprocity law fails quite seriously. An attempt was made to determine the extent of this failure by taking calibration spectra of seven hours exposure. While the results of these experiments were not sufficiently accurate to allow a correction to be made, it was estimated that the error was about 10% for the stronger bands and somewhat more for the weaker bands. The direction of the error was such that the weaker bands were actually more intense than measured. An additional error of unknown magnitude was introduced by the high and variable degree of fog on the high-speed plates used (Eastman type 103a-0)

On some plates, the scattered background from the arcs was subtracted. In order to distinguish this background from the

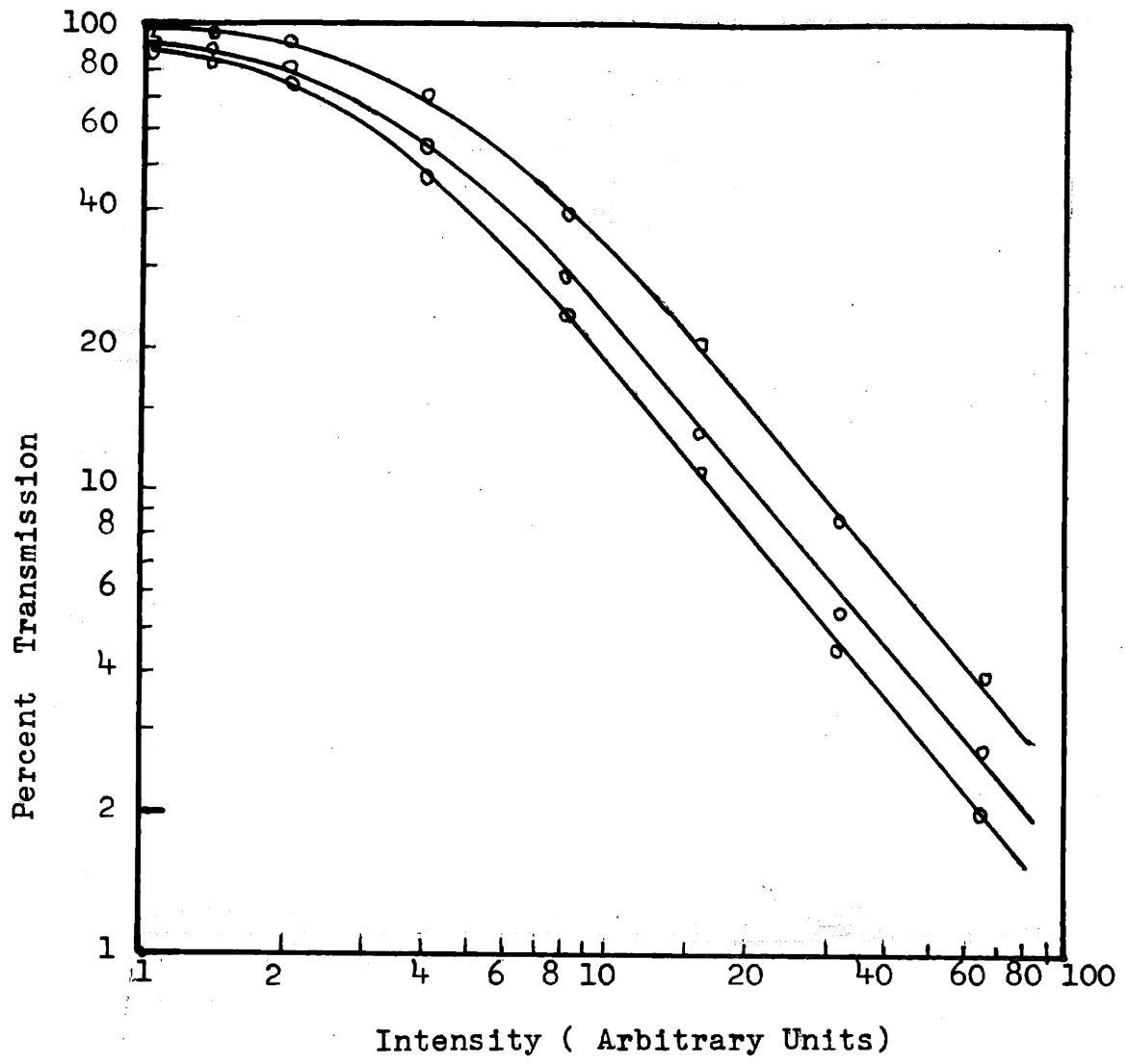


Fig. 9 Typical Calibration Curve for 103a-0 Plate

Raman scattering the following procedure was used: a yellow filter, Type K-2 (Wratten 8) was placed in the focal plane of the camera in such a position that only the exciting line passed through it. This filter absorbed the exciting line sufficiently so that its photographic image had a density of the same order as that of the scattered continuum. The spectrum of the arcs was then photographed and the ratio of the intensity of the exciting line to the background at various points determined.

With the K-2 filter still in place, a Raman spectrum was then photographed and the ratio of the intensity of the exciting line to that of exciting line in the arc spectrum plate was measured. It was assumed that the relative intensities of the scattered exciting line and the scattered background did not change from plate to plate. The intensity of the background on the Raman plate was found by multiplying the intensity of the background in the arc-spectrum plate by this ratio.

### Appendix III - Study on Cristobalite

Because the work of Simon and McMahon<sup>35</sup> indicated a closer relation between the spectra of cristobalite and vitreous silica than between those of quartz and vitreous silica, it was decided to make a Raman study of cristobalite. Unfortunately the only sample of cristobalite that could be obtained was in the form of a fine powder whose particle size was of the order of 1 to 10  $\mu$ . It appears doubtful that samples with substantially larger particle size exist.

The spectrum of the powder was observed by a modification of the method of Harrand<sup>14</sup>. In this method, light from a powerful mercury arc was purified by passage through a high-aperture monochromator. The sample was placed in a cell directly at the exit slit of the monochromator. The radiation emerging from the opposite side of the cell was then condensed on the entrance slit of a fast spectrograph. This emerging radiation is a mixture of scattered and transmitted Hg 4358 Å radiation plus any Raman scattering. By proper adjustment of the thickness of the sample, the amount of exciting line radiation may be made small and the intensity of the Raman scattering maximized.

In the present work, this method was somewhat modified. Filters, either praseodymium chloride solution, or interference filters, were used in place of the monochromator. The sample was wet with a solution of  $ZnCl_2$  whose reflective

index matched that of cristobalite in the region around 4500 Å. This allowed a much thicker layer of sample to be studied and permitted maximum possible transmission for the Raman scattering. The sample was contained in cells whose spacings varied from 0.2 to 1 cm. The cell was placed directly in front of the entrance slit of the spectrograph.

The first experiments were directed towards increasing the intensity of the Raman scattering. Accordingly an AH-4 arc was used in conjunction with a praseodymium chloride filter. This type of arc has high brightness and small size and could be effectively condensed on the sample cell. A small, fast Hilger spectrograph of low dispersion was used. These experiments were unsuccessful because of the high ratio of continuum intensity to exciting line(Hg 4358 Å) intensity in the AH-4 arc. The high degree of scattered light from the exciting line in the spectrograph and its low dispersion were further disadvantages.

The next series of experiments were concerned with increasing the purity of the radiation and decreasing the amount of Hg 4358 Å entering the spectrograph. To increase the purity, an AH-2 arc was substituted for the AH-4. The AH-2 arc operates at a lower pressure and gives a much

lower ratio of background intensity to exciting line intensity at some sacrifice in the latter. The radiation was collimated, passed through two multilayer interference filters and then condensed on the sample cell. The transmission of the two filters at 4358 Å was about 10% and at 4500 Å about 0.02%. These filters were considerably more effective than praseodymium chloride solution. The Zeiss spectrograph was used in these experiments. With this arrangement the spectrum of naphthalene powder could be photographed in 25 hours.

In some of the experiments on cristobalite, a cell containing an **alcoholic** solution of zinc tetraphenylporphine<sup>1</sup>, usually 1/10 saturated, was placed between the sample cell and the slit to reduce the intensity of the exciting line. This compound absorbs strongly in the region 4300 Å yet transmits quite well in the Raman region. However the region of high absorption is about 100 Å too far in the blue to absorb Hg 4358 Å effectively. A 1/10 saturated alcohol solution transmits about 25% at 4358 Å. Also the transmission in the Raman region is not as high as might be desired. Thus this filter was not too effective.

The spectrum of cristobalite was not detected for at least two reasons. First the scattering in the Zeiss spectrograph was still too high despite the precautions taken to cut down its effect. Second, the properties of interference

filters require their use in collimated light and thus greatly reduce the amount of Hg 4358 Å available at the sample cell.

In order to maintain a low ratio of continuum intensity to Hg 4358 Å and yet have high intensity at the sample cell, the final series of experiments utilized a low pressure mercury arc of the "Toronto" type. The grating spectrograph was used for these experiments because of its low scattering. With this arc and a condensing lens but with no filters except zinc tetraphenylporphine, it was possible to photograph the spectrum of naphthalene in 5 hours on the grating instrument. This spectrum was as intense as the 25-hour exposure mentioned above, although the grating camera is somewhat slower and the spectral slit width was only 1/4 that used above. The background on this plate was also lower indicating that the ratio of continuum intensity to Hg 4358 Å intensity was extremely low. Despite these improvements, exposures of 100 hours failed to detect the spectrum of cristobalite.

The difficulty was largely due to the small particle size since the spectrum of quartz with the same experimental arrangement and quartz powder of comparable particle size could not be detected. Harrand<sup>14</sup>, using the method mentioned at the beginning of this Appendix, has recently reported finding three lines of the Raman spectrum of cristobalite. One, a fairly strong line, is at  $470 \text{ cm}^{-1}$ , the other two lines

were very weak and came at 105 and 150 to 200  $\text{cm}^{-1}$ . This spectrum is obviously incomplete.  $\alpha$  -cristobalite has the symmetry of the space group  $D_4^4$  and the unit cell contains four  $\text{SiO}_2$  groups<sup>48</sup>. The usual analysis (see Herzberg, Ref. 17, Tables 18, 36, 55) shows that there are 29 Raman active fundamentals in  $\alpha$  -cristobalite.

Bibliography

1. Ball, R. H., Dorough, G. D., and Calvin, M.  
J. Am. Chem. Soc. 68, 2278 (1948)
2. Babcock, C. L., Barber, S. W., and Fajans, K.  
Ind. Eng. Chem. 46, 161 (1954)
3. Barber, S. W.  
*Owens-Illinois Glass Co.*  
Private communication
4. Barnes, R. B.  
Phys. Rev. 39, 566 (1932)
5. Barriol, J.  
J. Phys. radium 7, 209 (1946)
6. Bouhet, C.  
Compt. rend. 204, 1661 (1937)
7. Coblenz, W.  
Phys. Rev. 32, 125 (1906)
8. Crawford, M. F., Welch, H. L., and Harrold, J. H.  
Can. J. Phys. 30, 81 (1952)
9. Czerny, M.  
Z. Physik 53, 317 (1929)
- 9a. Edsall, J. T. and Wilson, E. B., Jr.  
J. Chem. Phys. 6, 124 (1938)
10. Florenskaya, V. A., and Pechenkina, R. S.  
Doklady Akad. Nauk S.S.R. 91, 59 (1953)
11. Gross, E. F., and Kolesova, V. A.  
Zhur. Fiz. Khim. 26, 1673 (1952)
12. Gross, E. F., and Romanova, M.  
Z. Physik 55, 744 (1929)

13. Haccuria, M.  
Bull. soc. Chim. Belges 62, 428 (1953)
14. Harrand, M.  
J. phys. radium 9, 81 (1948)
15. Harrand, M.  
Compt. rend. 238, 84 (1954)
16. Harrison, Lord, and Loofbourrow  
Practical Spectroscopy (Prentice-Hall Co., New York, 1948)
17. Herzberg, G.  
Infrared and Raman Spectra of Polyatomic Molecules  
(D. Van Nostrand, Inc., New York, 1945)
18. Hornig, D.  
J. Chem. Phys. 16, 1063 (1948)
19. Kemp, J. W., Jones, J. L., and Durkee, R. W.  
J. Optical Soc. Am. 42, 811 (1952)
20. Krishnan, R. S.  
Proc. Indian Acad. Sci. 22A, 329 (1945)
21. Krishnan, R. S.  
Proc. Indian Acad. Sci. 37A, 377 (1953)
22. Kujumzeliş, T.  
Z. Physik 97, 561 (1935)
23. Kujumzelis, T.  
Z. Physik 100, 221 (1936)
24. Landenberg, R.  
Ann. Physik 28, 104 (1927)
25. Liebisch and Rubens  
Berl. Ber., 199 (1919)

26. McMahon, H. O.  
J. Am. Ceram. Soc. 34, 95 (1951)
27. Morey, G. W.  
The Properties of Glass (Reinhold, New York, 1938) TABLE X.4
28. Narayanaswamy, P. K.  
Proc. Indian Acad. Sci., 28A, 417 (1948)
29. Nedungadi, T.K.M.  
Proc. Indian Acad. Sci. 11A, 86 (1940)
30. Rasetti  
Nuovo Cinento 2, 72 (1932)
31. Saksena, B. D.  
Proc. Indian Acad. Sci. 12A, 93 (1940)
32. Sangster, R.S.  
Ph. D. Thesis (M. I. T., 1951) DEPT. OF CHEMISTRY.
33. Simon, I.  
J. Optical Soc. Am. 41, 336 (1951)
34. Simon, I.  
Private communication
35. Simon, I., and McMahon, H. O.  
J. Chem. Phys. 21, 23 (1953)
36. Simon, I. and McMahon, H. O.  
J. Am. Ceram. Soc. 36, 160 (1953)
37. Stamm, R. F.  
Ind. Eng. Chem., Anal. Ed. 17, 318 (1945)
38. Stoicheff, B. P.  
Can. J. Phys. 32, 330 (1954)
39. Teller, E.  
Hand- und Jahrbuch der Chemischen Physik 2, 161 (1934)  
(Akademische Verlagsgesellschaft, Leipzig, 1934)

40. Vuks, M. F., and Ioffe, V. A.

Bull. Acad. Science URSS, classe des sciences tech.,  
3, 61 (1938)

41. Warren, B. E.

J. Am. Ceram. Soc. 17, 249 (1934)

42. Warren, B. E.

Chem. Rev. 26, 237 (1940)

43. Warren, B. E.

J. Applied Phys. 13, 602 (1942)

44. Warren, B. E. and Biscoe, J.

J. Am. Ceram. Soc. 21, 259 (1938)

45. Winston, H., and Halford, R. S.

J. Chem. Phys. 17, 607 (1949)

46. Wei, P'ei-Hsiu

Z. Krist. 92A, 355 (1935)

47. Welsh, H. L., Crawford, M. F., Thomas, T. R., and Love, G. D.

Can. J. Phys. 30, 577 (1952)

48. Wyckoff, R. W. G.

Crystal Structures, Vol. I, Chap. IV, text p. 26

(Interscience, New York, 1951)

49. Zachareasen, W. H.

J. Amer. Chem. Soc. 54, 3841 (1932)

## BIOGRAPHY

The author, a son of L. Howard Wilmot and Margaret B. Wilmot, was born on October 27, 1928 in Naugatuck, Connecticut. He attended the public school of that town graduating from Naugatuck High School in 1946. The following February he entered Rensselaer Polytechnic Institute where he majored in chemistry. After graduating from Rensselaer in January, 1951, he entered the Graduate School of the Massachusetts Institute of Technology in February, 1951. While at M.I.T., he held the positions of teaching assistant and research assistant in the Department of Chemistry. He is a member of Phi Lambda Upsilon and Sigma Xi.